IMPROVED BARRIER PROPERTIES OF PP/LDPE COMPOSITE FILM: EFFECT OF

MONTMORILLONITE AND POLY(LACTIC ACID)

Miss Supornpat Mooninta

จุฬาลงกรณ์มหาวิทยาลัย

CHULALONGKORN UNIVERSITY

A Thesis Submitted in Partial Fulfillment of the Requirements

for the Degree of Master of Science in Petrochemistry and Polymer Science

Field of Study of Petrochemistry and Polymer Science

Faculty of Science

Chulalongkorn University

Academic Year 2018

สมบัติปรับปรุงการต้านทานการซึมผ่านของฟิล์มคอมพอสิตพีพี/แอลดีพีอี: ผลของมอนต์มอริลโลไนต์และพอลิแล็กติกแอซิด

น.ส.ศุภรภัทร มูลอินต๊ะ

วิทยานิพนธ์นี้เป็นส่วนหนึ่งของการศึกษาตามหลักสูตรปริญญาวิทยาศาสตรมหาบัณฑิต
สาขาวิชาปิโตรเคมีและวิทยาศาสตร์พอลิเมอร์ สาขาวิชาปิโตรเคมีและวิทยาศาสตร์พอลิเมอร์
คณะวิทยาศาสตร์ จุฬาลงกรณ์มหาวิทยาลัย
ปีการศึกษา 2561

Thesis Title   IMPROVED BARRIER PROPERTIES OF PP/LDPE

COMPOSITE FILM: EFFECT OF MONTMORILLONITE

AND POLY(LACTIC ACID)

By   Miss Supornpat Mooninta

Field of Study   Petrochemistry and Polymer Science

Thesis Advisor   Associate Professor SIRILUX POOMPRADUB, Ph.D.

Thesis Co Advisor   Professor PATTARAPAN PRASASSARAKICH, Ph.D.

Accepted by the Faculty of Science, Chulalongkorn University in Partial

Fulfillment of the Requirement for the Master of Science

.... Dean of the Faculty of Science

(Professor POLKIT SANGVANICH, Ph.D.)

THESIS COMMITTEE

.... Chairman

(Assistant Professor WARINTHORN CHAVASIRI, Ph.D.)

.... Thesis Advisor

(Associate Professor SIRILUX POOMPRADUB, Ph.D.)

.... Thesis Co-Advisor

(Professor PATTARAPAN PRASASSARAKICH, Ph.D.)

.... Examiner

(Associate Professor NUANPHUN CHANTARASIRI, Ph.D.)

.... External Examiner

(Assistant Professor Suwadee Kongparakul, Ph.D.)

ศุภรภัทร มูลอินต๊ะ : สมบัติปรับปรุงการต้านทานการซึมผ่านของฟิล์มคอมพอสิตพีพี/แอลดีพีอี: ผลของมอนต์มอริลโลไนต์และพอลิแล็กติกแอซิด. (IMPROVED BARRIER PROPERTIES OF PP/LDPE COMPOSITE FILM: EFFECT OF MONTMORILLONITE AND POLY(LACTIC ACID)) อ.ที่ปรึกษาหลัก : รศ. ดร.ศิริลักษณ์ พุ่มประดับ, อ.ที่ปรึกษาร่วม : ศ. ดร.ภัทรพรรณ ประศาสน์สารกิจ

งานวิจัยนี้เป็นการปรับปรุงสมบัติของพอลิโพรพิลีน (PP) สำหรับการประยุกต์เป็นฟิล์มแบบชั้นเดียว โดยการผสมกับพอลิเอทิลีนความหนาแน่นต่ำ (LPDE) พอลิแล็กติกแอซิด (PLA) และมอนต์มอริลโลไนต์ (MMT) พอลิเมอร์คอมพอสิตเตรียมโดยการผสมแบบหลอมด้วยเครื่องอัดรีดแบบเกลียวคู่ และขึ้นรูปฟิล์มด้วยเครื่องอัดรีดแบบหล่อฟิล์ม การผสม LDPE ใน PP ช่วยเพิ่มสมบัติการยืดตัวที่จุดแตกหักและการทนแรงฉีกขาด พอลิเมอร์ผสม PP/LDPE ที่สัดส่วน 80:20 โดยน้ำหนัก ถูกเลือกสำหรับผสมกับ PLA และ MMT ปริมาณต่างๆ คอมพอสิตของ PP/LDPE/PLA/MMT มีค่ามอดูลัสที่เพิ่มขึ้น แต่การยืดตัวที่จุดขาดมีค่าลดลงตามปริมาณของ PLA และ MMT เพิ่มขึ้น สัณฐานวิทยาของนาโนคอมพอสิตตรวจสอบด้วยเทคนิคการกระเจิงของรังสีเอ็กซ์ (XRD) กล้องจุลทรรศน์อิเล็กตรอนแบบส่องกราด (SEM) และกล้องจุลทรรศน์อิเล็กตรอนแบบส่องผ่าน (TEM) สำหรับสมบัติการต้านทานการซึมผ่าน การเติม PLA และ MMT ในพอลิเมอร์ผสม PP/LDPE ลดความสามารถการซึมผ่านของแก๊สออกซิเจน และเพิ่มการซึมผ่านของไอน้ำ ดังนั้นคอมพอสิตฟิล์มของ PP/LDPE/PLA/MMT ที่อัตราส่วน 80/20/25/3 แสดงสมดุลที่ดีสำหรับสมบัติเชิงกลและการซึมผ่านของแก๊ส และมีศักยภาพในการใช้เป็นบรรจุภัณฑ์อาหาร นอกจากนี้ PP/LDPE/PLA/MMT คอมพอสิต ยังเป็นฟิล์มใหม่ที่มีประสิทธิภาพลดการสูญเสียน้ำหนักของมะเขือเทศที่อุณหภูมิต่ำ (14-20 ℃) ได้ดีกว่าฟิล์มพอลิโพรพิลีน

สาขาวิชา	ปิโตรเคมีและวิทยาศาสตร์พอลิเมอร์	ลายมือชื่อนิสิต ....
ปีการศึกษา	2561	ลายมือชื่อ อ.ที่ปรึกษาหลัก ....
		ลายมือชื่อ อ.ที่ปรึกษาร่วม ....

6072406723 : MAJOR PETROCHEMISTRY AND POLYMER SCIENCE

KEYWORD: POLYMER COMPOSITE, ORGNOMONTMORILLONITE, BARRIER FILM

Supornpat Mooninta : IMPROVED BARRIER PROPERTIES OF PP/LDPE COMPOSITE FILM: EFFECT OF MONTMORILLONITE AND POLY(LACTIC ACID). Advisor: Assoc. Prof. SIRILUX POOMPRADUB, Ph.D. Co-advisor: Prof. PATTARAPAN PRASASSARAKICH, Ph.D.

In this research, the properties of polypropylene (PP) were improved for single layer film application by incorporating low density polyethylene (LDPE), poly(lactic acid) (PLA) and montmorillonite (MMT). The polymer composites was prepared by melt blending using a twin screw extruder and the film was produced by cast film extruder. The addition of LDPE in PP improved the elongation at break and tear strength. The PP/LDPE blend at the ratio of 80:20 (w/w) was selected for blending with PLA and MMT and the PP/LDPE/PLA/MMT composite showed the increased tensile modulus while the elongation at break decreased with increasing PLA and MMT contents. The morphological structure of nanocomposite was examined by using X-ray diffraction (XRD) analysis, Scanning Electron Microscopy (SEM) and Transmission Electron Microscopy (TEM). For the barrier properties, the incorporation of PLA and MMT in PP/LDPE blend tended to decrease the oxygen permeability but increase the water vapor permeability. The 80/20/25/3 PP/LDPE/PLA/MMT composite film exhibited the good balance of mechanical and gas permeability properties and had a potential to be used as a food packaging. Moreover, the PP/LDPE/PLA/MMT composite as a new effective film could yield the decreased tomato loss weight at a low temperature storage (14-20 ºC) rather than PP film.

Field of Study:	Petrochemistry and Polymer Science	Student's Signature ....
Academic Year:	2018	Advisor's Signature ....
		Co-advisor's Signature ....

v

ACKNOWLEDGEMENTS

TABLE OF CONTENTS

LIST OF TABLES

LIST OF FIGURES

จุฬาลงกรณ์มหาวิทยาลัย
CHULALONGKORN UNIVERSITY

CHAPTER I

INTRODUCTION

1.1 Purpose of investigation

Barrier films in the packaging industries are carried out via multilayer co-extrusion, extrusion coating and adhesive lamination process. There are complex and expensive technologies and the final product are not recyclable or biodegradable. Blending polymer is a simple technique to enhance the property of pure polymer for using in single layer barrier film. The blends of commodity and barrier polymer are the alternatives to improve the barrier properties and lead to a low-cost product.

Polypropylene (PP) is a commodity polymer with suitable mechanical properties, transparency, satisfactory hear resistance and good barrier to moisture, but its low flexible and poor barrier to oxygen limits its applications. Linear low-density polyethylene (LDPE) is widely used as important packaging industries due to its excellent properties such as high flexible, impact resistance and chemical resistance. PP/LDPE blending with the high ratio of PP can improve flexible property and tear resistance of polypropylene and maintain the strength properties [1, 2]. Besides, Poly (lactic acid) (PLA) is well-known biodegradable polyester with significantly lower oxygen permeability and poor barrier to moisture as compared to PP. Meanwhile, polymer/clay nanocomposites have been attracting great interest because of their improving the mechanical properties, thermal properties and gas barrier properties of polymer [3, 4].

Therefore, blending of PP, LDPE and PLA as green polymer can be a good alternative for solving their permeability problem, and incorporation of clay can improve these properties. In this research, the effect of LDPE, PLA and organoclay blend composition on mechanical properties, thermal properties and permeability of PP film was investigated. The polymer blend and polymer nanocomposite with enhanced mechanical and barrier properties were tested with tomato storage for studying the extent shelf life food packaging.

1.2 Research objective

1.2.1 Study the effect of PP, LDPE, PLA and montmorillonite ratio on the mechanical properties, thermal properties and permeability properties.

1.2.2 Study the effect of packaging film on the tomatoes storage and shelf life at 14-20 ºC.

1.3 Scope of the investigation

The PP/LDPE/PLA/MMT composite was prepared at various ratios. The effect of PP, LDPE, PLA and montmorillonite ratio on the mechanical, thermal and permeability properties was studied. The experimental procedures were carried out as follows:

1. Survey literature and study the research work.
2. Prepare the PP/LDPE/PLA/MMT composite by using twin screw extruder at various ratios of PP, LDPE, PLA and MMT.
3. Prepare composite films by using cast film extruder machine.
4. Investigate the mechanical properties of PP/LDPE/PLA/MMT composite films.
5. Investigate the thermal properties of PP/LDPE/PLA/MMT composite.
6. Investigate the permeability properties of PP/LDPE/PLA/MMT composite film.
7. Investigate the morphology of PP/LDPE/PLA/MMT composite films.
8. Investigate the physiological loss weight and appearance of tomato in composite film packaging and the biodegradation of composite films.
9. Summarize the results.

1.4 Expected beneficial outcome(s) from the thesis

The optimum compositions of polymer composite with good mechanical and barrier properties for food packaging film.

CHAPTER II

THEORY AND LITERATURE REVIEWS

2.1 Polypropylene (PP)

PP is prepared via a polymerization of propylene, a gaseous by product of petroleum refining. The polymerization process of propylene is carried out by a catalyst system under carefully heat and pressure controlled. The steric arrangement of the methyl groups attached to every alternate carbon atom in the backbone chain. The molecular structure that all the methyl groups are on the same side of the chain molecule, the product is referred to an isotactic PP. A PP structure where the alternate pendant methylene groups are on opposite sides of polymer backbone chain is known as a syndiotactic PP. While, the structure where the pendant groups are randomly located in a manner on the polymer backbone is knows as an atactic form (Figure 2.1).

isotactic polypropylene

syndiotactic polypropylene

atactic polypropylene
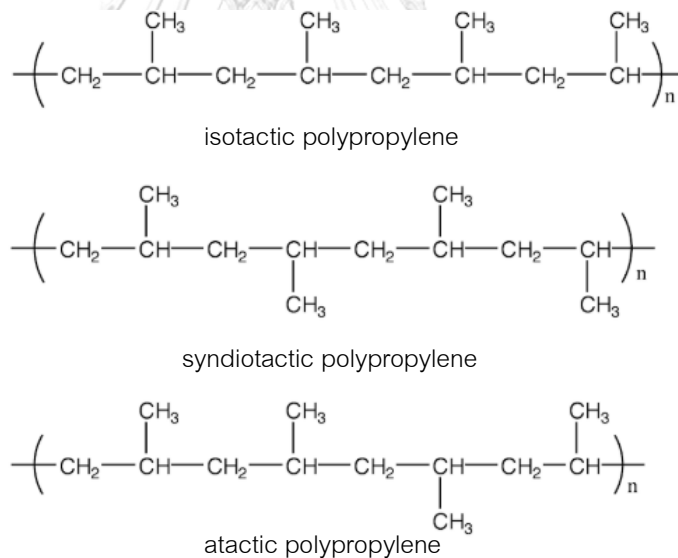
Figure 2.1 PP polymer molecule in isotactic, syndiotactic and atactic forms.

PP is very popular as a high-volume commodity plastic. It is higher stiffness at lower density and higher temperature resistance than polyethylene (PE) (Table 2.1). In addition, PP offers good chemical resistance, good fatigue resistance, low water vapor transmission, medium gas permeability, transparency and easy to process by injection molding and extrusion. The major disadvantages of unmodified PP have higher thermal

expansion and lower impact strength than high impact polystyrene (HIPS), poly(vinyl chloride (PVC) and acrylonitrile butadiene styrene (ABS) [5].

Table 2.1 Comparison of unmodified PP with other materials

Property	PP	LDPE	HDPE	HIPS	PVC
Flexural modulus (GPa)	1.5	0.3	1.3	2.1	3.0
Tensile strength (MPa)	33	10	32	42	51
Specific density	0.905	0.92	0.96	1.08	1.4
Specific modulus (GPa)	1.66	0.33	1.35	1.94	2.14
HDT at 0.45 MPa (ºC)	105	50	75	85	70

2.2 Low density polyethylene (LDPE)

LDPE is a thermoplastic produced from the monomer ethylene. The chemical structure of LDPE is shown in Figure 2.2. The first grade of polyethylene was produced in 1933. The density range for LDPE is 0.91 to 0.94 g/cm^3. LDPE has well the toughness, flexibility, resistance to chemicals and weather, and low water absorption properties. It is a corrosion-resistant, low density extruded material that provide low moisture permeability. The disadvantages of LDPE are its low stiffness, strengths and maximum operating temperature, high gas permeability, poor UV, and flammability resistance.
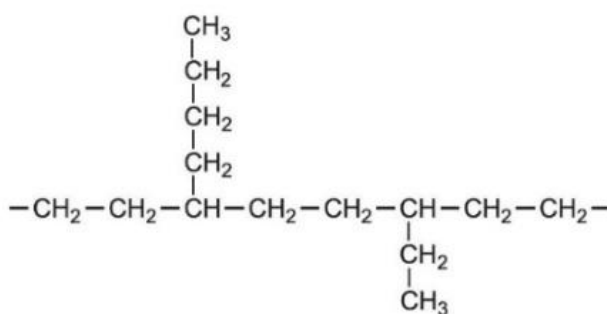
Figure 2.2 Chemical structure of LDPE [6].

The main market of LDPE is in high clarity product, which includes produce bags, bakery film, textile and paper overwrap. The application of LDPE has become solidly established for the following PE melt flow index (MFI) ranges as shown below:

MFI 0.3   for sack-and heavy-duty film, shrink film

MFI 0.7 to 1   for carrier bags, general packaging film, refuse bag film

MFI 2   for thin films, lamination film, thin shrink films

MFI 4   for thin films

(Note: MFI at 190 ºC/2.16N) in g/10 min) [7].

2.3 Poly(lactic acid) (PLA)

PLA is a rigidity an clarity thermoplastic material similar to polystyrene (PS) or poly(ethylene terephthalate) (PET). The PLA production is carried out by polycondensation directly from its basic building block lactic acid or ring opening polymerization of lactide. The lactic acid monomer can be derived by sugars fermentation from carbohydrate sources such as sugarcane, corn, starches, or tapioca.

The properties, crystallization, processing and degradation behavior of PLA depend on the stereochemical structure and isomer composition of the polymer chain, in particular the ratio of the L- to the D-isomer of lactic acid. The properties of PLA can be modified by copolymerization of mixture of L-lactide, meso-lactide and D-lactide (Figure 2.3) resulting in high molecular weight amorphous or semi-crystalline polymers with a melting point in the range from 130 to 185 ºC [8].
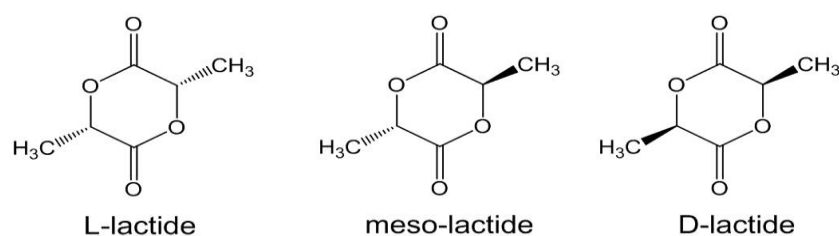
Figure 2.3 Dimeric lactide isomers [9].

Table 2.2 PLA properties [10]

Properties	Nominal Value
Density (g/cm^3)	1.22-1.30
Tensile modulus (MPa)	889-3647
Tensile strength (MPa)	61-62
Elongation at break (%)	0.5-19
Flexural modulus (MPa)	2275- 4495
Notched Izod Impact at 23 ºC (ft·lb/in)	0.30-0.88

PLA is one of the most promising biodegradable polymers is a material that derived from annually renewable resources. Mostly, PLA was initially used to medical application due to it high cost and biocompatibility with the human body. Some of the applications of fiber grade PLA are restorable sutures, implants for orthopedics, thermoforms, surgical materials, containers, oriented and blown films, fibers and textiles.

2.4 Clay

Clay mineral are the phyllosilicate or sheet silicate family of minerals. The layered structures composed of tetrahedral silica (SiO$_4$) polymeric sheets attached with octahedral sheets (containing aluminum (Al), magnesium (Mg), iron (Fe), alkali metals and alkaline earths). These minerals are layered-type aluminosilicates which are formed of silicate mineral that present on the Earth's surface as a result of chemical weathering [11].

2.4.1 Type of clay mineral

There are two major types of clay minerals are 1:1 and 2:1 type mineral.

a) 1:1 type mineral

The 1:1 clay mineral type consists of one tetrahedral sheet and one octahedral sheet. The thickness of two sheets are approximately 7 Å as shown in Figure 2.4.
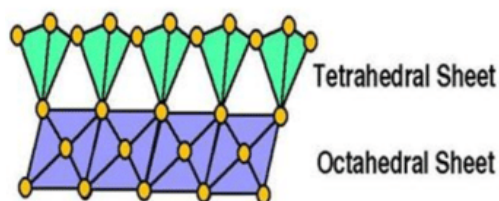
Figure 2.4 1:1 type mineral [12].

A kaolin mineral is one of 1:1 type mineral. The structure consists of a single silica tetrahedral sheet and a single alumina octahedral sheet combined in a unit. Kaolin group includes the mineral Chrysotile, Amesite, Lizardite, Kaolinite, Dickite and Halloysite.

b) 2:1 type mineral

The three sheets or 2:1 layer lattice silicates consist of two silica tetrahedral sheets between which is an octahedral sheet. These three sheets form a layer approximately 10 Å thick as shown in Figure 2.5.
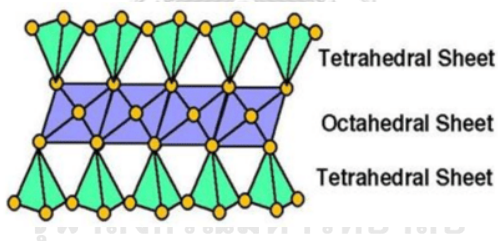
Figure 2.5 1:1 type mineral [12].

The 2:1 layer typed aluminosilicate can be classified into the following subgroups: pyrophyllite, smectite, vermiculite, illite, mica, brittle mica, and chlorite [13]. There is the difference of their layer charge density as presented in Table 2.3.

Table 2.3 Classification of clay in phyllosilicate types [14]

Layer type	Group	Species
1:1	Kaolinite-serpentine (x~0)	Chrysotile, Amesite, Lizardite, Kaolinite, Dickite, Halloysite
2:1	Pyrophyllite-talc (x~0)	Talc Pyrophyllite
	Smectite (x~0.2-0.6)	Saponite, Hectorite, Sauconite, Montmorillonite, Bentonite, Beidellite
	Vermiculite (x~0.6-0.9)	Trioctahedral vermiculite Dioctahedral vermiculite
	Illite (x<0.9-0.6)	
	Mica (x~1.0)	Biotite, Phlogipite, Lepidolite, Muscovite, Paragonite
	Brittle mica (x~2.0)	Clintonite, Anandite, Margarite
	Chlorite (x variable)	Common name based on Fe^{2+}, Mg^{2+}, Mn^{2+}, Ni^{2+}, Ponbassite, Sudoite, Codecite (Li)

where x means the charge per formula unit

2.4.2 Montmorillonite

Montmorillonite was widely used in polymers. It is a group of smectite clay that can absorb water. The layered structure consists with aluminium octahedron sandwiched between two layers of silicon tetrahedron. The paricles are plate-shape with each layered sheet is slightly less than 1 nm thin (10 Å) with an average dimensions extending to around 1 μm or 1000 nm. Therefore, the aspect ratio is extremely high average of 1000 to 1 and the surface area is in excess of 740 m^2/g.
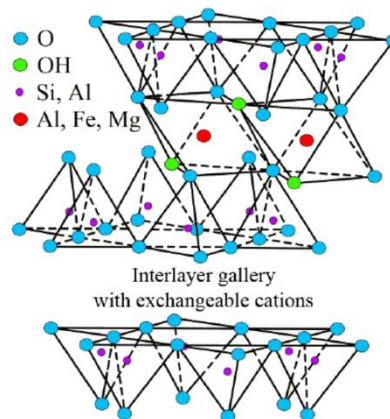
Figure 2.6 Structure of the smectite mineral, montmorillonite [15].

Montmorillonite is one in smectite group which has a low thermal expansion coefficient and a high gas barrier property. Stacking of this structure leads to a regular weak dipolar of van der waals interaction between the layers. The hydrated sodium of potassium ions residing in the interlayer spaces counterbalance the negative charge in each layer that lead to isomorphic substitution. Typically, montmorillonite clay is hydrophilic; hence it is not inherently compatible with most polymers and must be modified the surface chemistry of clay to make its more hydrophobic.

2.4.3 Organoclay

The term organoclay mainly denoted a family of hydrophobic materials that are obtained by modifying clays and clay minerals with various organic compounds through an intercalation process. Organoclay is the hybrid material that was synthesized by ion exchange reaction between various organic cation and cation residing (Na^+, Ca^{2+}, or K^+) in the gap between silicate layers, which was termed as the interlayer gallery. The organic cation typically uses quaternary alkylammonium cations that can expand the interlayer space and make the silicate hydrophobic. The treatments minimize the attractive forces between the agglomerated platelets as shown in Figure 2.7. The organic cations promoted the compatibility of the silicate layers with the polymer matrix [16].
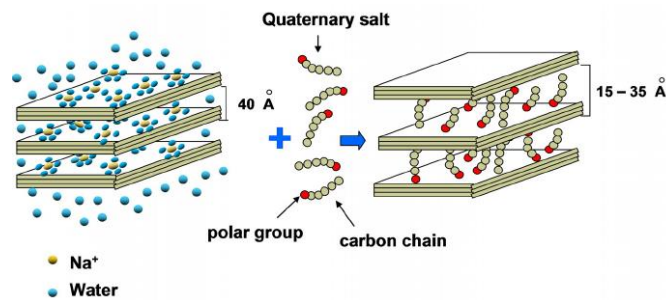
Figure 2.7 Clay surface treatment [17].

2.5 Nanocomposite

Composite materials are a material made from at least two distinctly dissimilar materials to produce a new material different property. For conventional composites, phase mixing typically occurs on a macroscopic (µm) length scale. In contrast, a nanocomposite is formed when phase mixing occurs on a nanometer length scale. The overall properties of a composite material are determined not only by the parent components but also by the composite phase morphology and interfacial properties. Nanocomposites usually exhibit improved performance properties compared with conventional composites owing to their unique phase morphology and improved interfacial property.

2.5.1 Nanocomposite preparation

a) Direct mixing (Melt mixing)

Direct mixing takes advantage of well-established polymer processing techniques. Nanocomposites can be sufficiently rapid processed in a twin-screw extruder. The strategy is to blend a molten thermoplastic with an organosilicate in order to optimize the polymer/layered silicate interaction.

b) Solution mixing

Solution mixing is the method base on a solvent system which both the polymer and the nanoparticles are dissolved or dispersed in solution. This technique reduces particle agglomeration. The nanoparticle/polymer solution can then be cast into a solid, or can be separated from solution by solvent evaporation of precipitation.

c) In-Situ polymerization

In this technique, nanoscale particles are dispersed in the monomer or monomer solution, and the resulting mixture is polymerized by standard polymerization methods.

2.5.2 Nanocomposite types

Generally, polymer/layered silicate composites are ideally divided into three types.

a) Conventional composite and nanocomposite, the clay nanolayers is retained polymer matrix when mixed with the polymer, but polymer chain did not insert into the clay galleries (Figure 2.8a). Consequently, the clay fraction in conventional clay composites plays little of no functional role and acts mainly as a filling agent for economic considerations. In conventional clay composite can normally improve in modulus, but this reinforcement benefit is usually accompanied with a decreasing in other properties, such as elasticity and strength.

b) Intercalated nanocomposites (Figure 2.8b) are formed when one or a few polymers molecular insert into the galleries of clay with fixed interlayer spacing. The intercalated type of polymer-clay hybrid has been formed to have highly extended single chains confined between the clay sheets, within the gallery regions. The clay sheet retains a well ordered, periodic and stacked structure.

c) Exfoliated nanocomposite (Figure 2.8c) are formed when the molecular polymers can insert into the clay interlayer leading to disperse of silicate nanolayers in the polymer matrix. The separation between the exfoliated nanolayers may be uniform or variable. However, the average distance between the segregated layers being depend on the clay loading. Exfoliated nanocomposites show greater phase than intercalated nanocomposites. More importantly, each nanolayer in an exfoliated nanocomposite contributes fully to interfacial interaction with the matrix that provide the especially effective in performance properties and improving the reinforcement of clay composite materials [18].
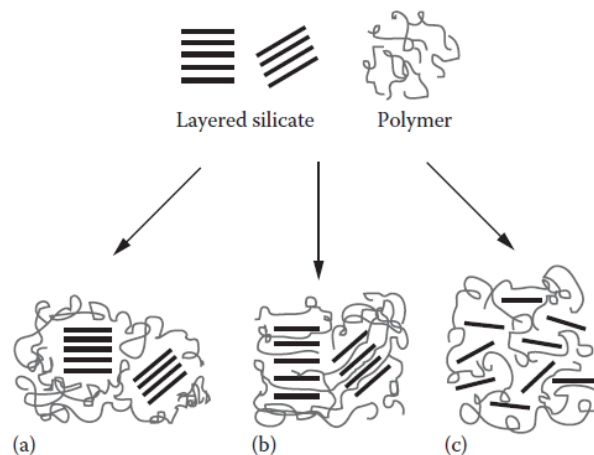
Figure 2.8 Illustration of different types of composites that can arise from the interaction between layered silicates and polymers. (a) Conventional composite (b) Intercalated nanocomposite (c) Exfoliated nanocomposite [19]

2.6 Polymer blends

Polymer blend is a mixture of at least two polymers that have been blended together to create a new material with different physical and mechanical properties. Polymer blend technique has attracted much attention for developing polymeric material because of an easy and cost-effective method for commercial applications. In other words, the properties of the blends can be manipulated according to their end use by correct component selection. Mostly polymers are widely used in blending of two semi-crystalline polymers or blending of semi-crystalline polymer with an amorphous polymer.

2.6.1 Miscible and immiscible polymer blends

Generally, polymer blends are classified into either homogeneous (miscible) or heterogeneous (immiscible) blends. For example, poly(phenylene oxide) (PPO-poly(styrene) (PS) and poly(methyl methacrylate) (PMMA)-poly(styrene-acrylonitrile) (SAN) are miscible blends, while PP-PS and PP-PE are immiscible blends. Miscible blends are homogenous to the polymer segmental level and usually optically transparent. Single phase blends also undergo phase separation that is usually brought about by variation in the composition of the mixture temperature, or pressure.

Generally, polymer blends can be completely miscible, partially miscible or immiscible, depend on the value of ΔG_m.

The free energy of mixing is given by

$$\Delta G_m = \Delta H_m - T\Delta S_m \qquad (2.1)$$

For miscibility (binary blend), the following two conditions must be satisfied: the first condition $\Delta G_m < 0$; and the second condition

$$\left(\frac{\partial^2(\Delta G_m)}{\partial \emptyset_i^2}\right)_{T,p} > 0 \qquad (2.2)$$

where ΔG_m is the Gibbs energy of mixing, $\emptyset$ is the composition, where $\emptyset$ is usually taken as the volume fraction of one of the components. ΔS_m is the entropy factor that is a measure of disorder or randomness and always positive. Therefore, ΔS_m is favorable parameter for mixing or miscibility especially for low molecular weight solutions. In contrast, polymer solutions have polymers with a high molecular weight and hence the enthalpy of mixing (ΔH_m) is also a deciding factor for miscibility [20].

The biggest thing that affects the morphology of an immiscible blend is the amount of two polymers. Polymer A and Polymer B are the immiscible blend. Blending polymer A at higher content than polymer B leads to the little spherical polymer B. The spheres of polymer B are separated from polymer A matrix (Figure 2.9). In such a case, polymer A is called the major component and polymer B is called the minor component. However, the ratio of polymer B is increased to the immiscible blend. The spheres will be larger, and become joined together to the continuous phase with increasing polymer B content. The polymer A phase and the polymer B phase are co-continuous. Moreover, polymer B is added more than polymer A resulting that the polymer A becomes the spheres domain, then polymer A is the minor component and polymer B is the major component.

relative amount of polymer B in the immiscible blend
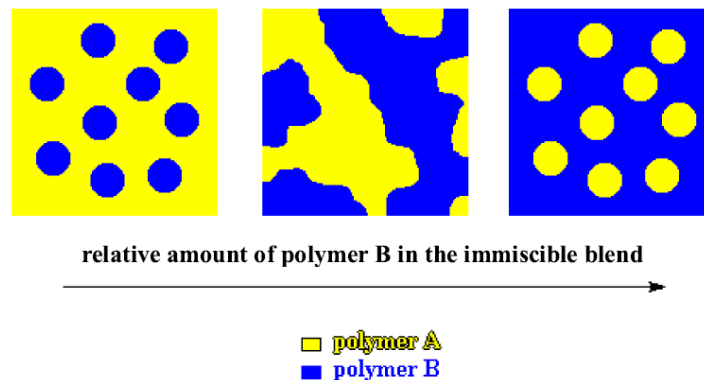
☐ **polymer A**
■ **polymer B**

Figure 2.9 Representative the morphology of polymer immiscibility blend [21].

2.6.2 Factors in miscibility and Immiscibility

a) Polarity

Polymers that are similar in structure or polarity are less to repel each other and more likely to form miscible blends. In general, the difference polarities produce immiscibility blend.

b) Specific group attraction

Polymers that are drawn to each other by hydrogen bonding, Ion-dipole, charge transfer, acid-base, donor-acceptor adducts, or transition metal complexes are less common. However, they are likely to the miscibility blen when occur the attractions.

c) Ratio

Two polymers mostly appear immiscible blend at a fairly equal ratio. However, a small amount of one polymer may be possible to soluble in a large amount of the other polymer, as understood in conventional phase rule. This consideration is very important in natural compatibility.

d) Molecular weight

Lower molecular weight permits greater randomization on mixing and therefore greater gain of entropy, which favors miscibility. Moreover, the similar molecular weight polymers are more miscible, while polymers of very different molecular weights may occur the immiscible blend, even if they both have the same composition.

e) Crystallinity

The polymer crystallizes forms a two-phase system. Therefore, a polymer crystallizes in polymer blend that exhibit another phase to the system. If both polymers in a blend crystallize, they will usually form two separate crystalline phases. Thus, it is difficult to co-crystalline of the two polymers in a single crystalline phase [22].

2.6.3 Compatibility in polymer blends

In general, the compatibility between the polymer phases is considered the heterogeneous polymer blend properties. The interface interaction between the polymer phases measurement by the interfacial tension. The miscible blend has the interface tension approaching zero. In other words, the miscible blend is strong interaction of interphase. The high interfacial tension lead to phase separation by agglomerate of minor component particle resulting the decreased mechanical properties. The interfacial tension can be reduced by the addition of interfacial agents known as compatibilizers, which are generally molecules with hydrophilic and hydrophobic regions that can localize to the interfaces between the two polymers phase, causing the reduced interfacial tension and the increased polymer compatibility. Compatibility lead to reduce size of dispersed particles, enhanced the phase stability, and increase mechanical properties. The physical properties of miscible and compatibilized blends can be characterized by using technique such as thermogravimetric analysis, differential scanning calorimetry, dynamic mechanical thermal analysis, microscope, and universal testing machines [20].

2.7 Barrier properties

The barrier properties of plastics indicate their resistance to diffusion and sorption of substances such as gases, flavor and aroma compounds. The solution and transport behavior of low MW substances in plastics has become increasingly important in recent years with the widespread and expanding use of polymer films and rigid plastics for food packaging. The selection or development of plastics for food

packaging applications with stringent design specifications relating to their solution and diffusion behavior requires knowledge and appreciation of the many factors which affect those phenomena.

The integrity of package is important factor that protect foods from gas and vapor exchange with the environment (including their seals and closures) and including the barrier properties of the packaging materials themselves. There are two processes that gases and vapors may pass through polymeric materials:

1. A pore effect: the gases and vapors can flow through micropores, pinholes and cracks in the materials.

2. A solubility-diffusion effect: the gases and vapors dissolve on the polymer surface, then they diffuse through the polymer because a concentration gradient and evaporate at the other polymer surface. This "solution-diffusion" process (also known as "activated diffusion") is described as true permeability.

Barrier properties are determined by the steady-state rate of mass transport through the films. The permeability coefficient, P, can be defined by

$$P = \frac{(volume\ of\ permeate) \cdot (film\ thickness)}{(area) \cdot (time) \cdot (pressure\ drop\ in\ film)} \qquad (2.3)$$

The permeability coefficient is not only a function of the chemical structure of the polymer, but it also depends on many physical factors such as density, crystallinity, orientation, cross-linking, plasticizers, temperature and moisture sensitivity. Thus, film properties comparation should be tested at the same conditions as soon as possible [18]. The examples permeability coefficient of various polymer was presented in Table 2.4.

Table 2.4 Broadly representative permeability coefficients of various polymers and permeants at 25°C and 0% relative humidity (RH) unless indicated otherwise [18].

Material	Permeability $((10^{-10}$ (mL at STP) cm)/ (cm^2 s (cm Hg))		
	O_2	CO_2	H_2O (90% RH)
LDPE	3.0-6.7	13-28	80
HDPE	0.6-1.1	1.7-4.5	13
PP	0.9-2.3	9.2	57
PVC	0.005-0.12	0.03-1.0	156-275
PS (oriented)	1.1-2.7	8.8-10.5	11-1,800
EVOH (33% ethylene)	0.00012	0.00036	-
PLA (98% L)	0.11-0.56	1.88	3,000

2.7.1 Variables affecting permeability

a) Chemical structure of polymer

The barrier properties of films depend on the specific molecular structures of the polymer involved. A structure that provides a good barrier to water vapor may provide a poor gas barrier. For example, nonpolar hydrocarbon polymers such as polyethylene or polypropylene have excellent water vapor barrier but poor gas barrier properties, the latter property improving as the density of the polyethylene increases. In contrast, highly polar polymers such as those containing hydroxyl groups (PAs and EVOH copolymers) are excellent gas barriers but poor water vapor barriers. Furthermore, their effectiveness as gas barriers is reduced when the polymer is plasticized by water. Moreover, the number or size of cavities in a polymer or renders chain segments more mobile increases the rate of diffusion.

Orientation often leads to lower permeability as it can increase packing density. However, more stretching does not always lead to molecular chain orientation and may in fact result to void formation that increases permeability. The permeability can be reduced by increasing crystallinity because the crystal regions are impenetrable in most semi-crystalline polymers and movement must occur around the crystallites.

b) Pressure

Permeability is independent of the diffusing gas pressure. This is also true if diffusing gases and vapor do not interaction with polymer. However, the permeability depend on the pressure where there is strong interaction. In general, the permeability increases with increasing the pressure.

c) Temperature

The temperature dependence of the solubility (S) over relatively small ranges of temperature can be represented by an Arrhenius-type relationship:

$$S = S_0 e^{-\frac{\Delta H_s}{RT}} \qquad (2.4)$$

where ΔH_s is the heat of sorption. For the permeant gases, ΔH_s is small and positive and therefore S slightly increases slightly with temperature. For easily condensable vapors, ΔH_s is negative due to the contribution of the heat of condensation, and thus S decreases with increasing temperature.

The temperature dependence of the diffusion (D) can also be represented by an Arrhenius-type relationship as in the following:

$$D = D_0 e^{\frac{-E_d}{RT}} \qquad (2.5)$$

where E_d is the activation energy for the diffusion process. E_d is always positive, thus D increases with increasing temperature.

From the two previous equations, it follows that

$$P = P_0 e^{\frac{-E_P}{RT}} \qquad (2.6)$$

$$= (D_0 S_0) exp[-(E_d + \Delta H_s)/RT] \qquad (2.7)$$

where $E_P = (E_d + \Delta H_s)$ is the apparent activation energy for permeation.

It follows that the P of a specific polymer-permeant system may increase or decrease with the increases of temperature depending on the relative effect of temperature on S and D. Generally, S increases with increasing temperature for gases and decreases for vapors and D increases with increasing temperature for both gases and vapors. Therefore, P of different polymers determined at one temperature may not be in the same relative order at other temperatures.

d) Humidity

Hydrophilic polymer such as polyamides and ethylene vinyl alcohol copolymer (EVOH) strongly absorb water from humid air due to contain polar groups and hydrogen bonding capability. Therefore, one can determine a water sorption isotherm for the polymer; that is, the equilibrium moisture content at any temperature and humidity condition. The presence of the water vapor in the polymer effect on the permeation of other gases and vapors through the polymer. In most cases, the permeation rate increase with higher water sorption because the water acts as a plasticizer and increases the free volume of polymer.

2.7.2 Transmission rate

Permeability of polymers to water vapor, gases and organic compounds are usually presented in the transmission rate. The water vapor is often presented in the term WVTR (water vapor transmission rate) . For gases, the general term GTR (gas transmission rate) is used as well as the specific terms OTR or O_2TR (oxygen transmission rate) or O_2GTR (oxygen gas transmission rate according to ASTM standards) and CDTR or CO_2TR (carbon dioxide transmission rate) where appropriate.

a) Oxygen gas transmission rate

The oxygen transmission rate is the measurement of the amount of oxygen gas that passes through a substance at specified condition of temperature and relative humidity (RH). The transfer of oxygen from the environment has an important effect on quality and shelf life of food. Oxygen cause food deterioration such as lipid and vitamin oxidation, leading to sensory and nutrient changes.

b) Water vapor transmission rate

Water vapor permeability of a polymer depend on the polymer polarity, crystallinity, orientation, molecular weight, chain symmetry, and temperature. WVTR is the standard measurement for determined moisture resistance of films. Lower WVTR values indicate better moisture protection. Only values reported at the same

temperature and humidity can be compared, because both of these parameter effect the water vapor transmission rates [20].

2.8 Film casting process

The production of films of thermoplastic polymers is a large activity of the polymer processing industry. The products are primarily used in the packaging industry for food or consumer products. Quite frequently, the properties of various polymers need to be combined by coating, lamination, or co-extrusion.
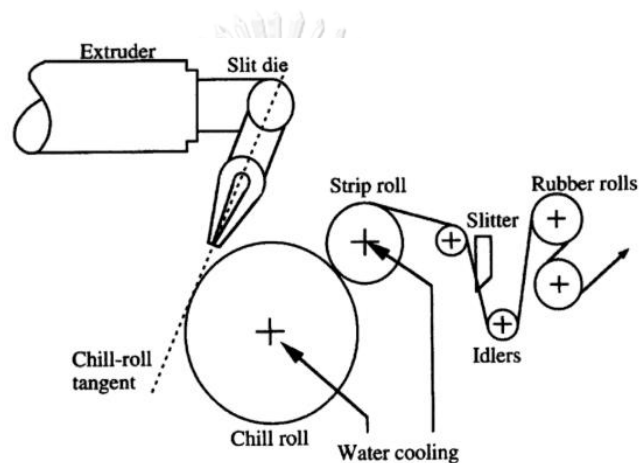
Figure 2.10 Chill roll film process.

There are two typical configurations for film casting: chill roll casting film and water bath casting [23]. The chill roll casting process for manufacturing film shown in Figure 2.10, is applicable to a wide range of thermoplastics, including such as PP, polyamides, and polyesters which are rarely converted into film by any other method. In the chill roll casting process, the extruder forces a thin web of melt through a slot die onto a rotating chill roll, which both cools the film and draws it away from the die at a controlled rate to stretch and thin down the film in the machine direction. Cooling of the film is completed on additional cooling roll before the edges are trimmed and the product wound up. A chill roll casting line therefore consists of five basic elements: the extruder, slot die, casting roll, cooling roll, haul-off (nip) rolls and the wind up.

The cooling of the film with cast extrusion is highly efficient more than the blown film process. This provides the higher production line speeds resulting in higher production rates with superior optical properties of the product. The thickness distribution of film in the machine cross direction with cast process is more uniform than in the blow film process because of the lower degree of draw and orientation (with variations that could be as low as ± 1.5%). However, the film mechanical properties in the machine cross direction are lower when compared with the blown film process due to the higher level of molecular chain orientation of blown film process [24].

2.9 Literature review

Kadhim *et al.* [1] studied the properties of PP/LDPE polymer blend. The superior was obtained at PP/LDPE ratio 75:25 w/w. The tensile strength of PP/LDPE blend was decreased with increasing LDPE content due to the phase separated effect morphology of LDPE form PP and the nature of LDPE is more flexible than PP.

Mofokeng *et al.* [2] investigated the influence of blend ratio on the morphology, mechanical, thermal and rheological properties of PP/LDPE blends. The morphology of blend was composed of the major matrix and minor matrix phase. The blends containing lower 20 wt% of either phase exhibited partial miscibility but the phase was immiscible at higher contents. The melting temperature of blend polymer was not significantly affected by blending but the crystallization of PP was delayed by incorporation LDPE. The thermal stability of PP/LDPE blend implied the enhancement with the addition of the more LDPE. The tensile modulus of the blends decreases with increasing amount of LDPE. However, the modulus was only affected at additions over 10 wt% of LDPE. The elongation at break of blend with LDPE content 20 to 40 wt% was increased due to the phase separated morphology effect with increasing LDPE concentration. The PP/LDPE blend with ratio 80:20 offed a balance among the mechanical properties that was essential for flexible packaging applications.

Ebadi-Dehaghani *et al.* [3] studied on oxygen gas permeability of PP/PLA/clay nanocomposite. The result indicated that the permeation was highly dependent on blend composition, clay loading and state of clay dispersion. The uniform distribution of PLA in PP enhanced the tortuous path and improved the oxygen barrier. The appropriate PP/PLA ratio was 75:25. In addition, the organoclay that gave the extent of exfoliation in the polymer was important for improving the barrier properties of the blend but the oxygen permeability was decreased with increasing oraganoclay content up to 5 wt% due to the aggregating phenomenon.

Ebadi-Dehaghani *et al.* [4] studied the experimental and theoretical analyses of mechanical properties of PP/PLA/clay nanocomposite. The SEM micrographs demonstrated that PLA as the spherical domains dispersed in the matrix of the blends. The tensile modulus and strength of blend were increased with increasing PLA content but elongation at break and impact strength were decreased. In addition, compatibilizer improved the distribution and size of spherical domains of PLA. As the result, tensile modulus, elongation at break and impact strength were increased. Whlie the incorporation of organoclay led to significant increase in tensile modulus and decrease in elongation at break due to that the nanoparticle can act as stress concentration points. However, compatibilizer change the properties differently. The tensile modulus decreased but elongation at break increased because of the localization of the nanoparticles from PLA to PP phase and greater exfoliation of organoclay.

Chang *et al.* [25] studied the structure of blown film from blends of high density polyethylene (HDEP) and high melt strength polypropylene (hmsPP). The result indicated that the tensile strength of blend was between the tensile strength of hmsPP and HDPE. The tensile strength was decreased with the increasing HDPE but the elongation was significantly increase.

Abdel-Hamid *et al.* [26] studied the thermo-mechanical characteristics of thermally aged PP/LDPE blend. It was found that the tensile strength, tensile modulus and hardness of polymer blend were decreased with increasing LDPE content but

elongation were increased. The addition of LDPE to the PP by weight ratio of 25:75 reduced the percentage crystallinity by 20%.

Pivasaart *et al.* [27] investigated the effect of compatibilizer on PLA/PP blend for injection molding. As the result, the amount of PP-g-MAH did not affect the thermal properties of the polymer blends but tensile strength was slightly decreased with increasing PP-g-MAH increasing. The tensile strength of polymer blend was increased with increasing amounts of PLA.

Pannirselvan *et al.* [28] investigated the oxygen barrier property of PP-polyether treated clay nanocomposite. Nanocomposites prepared with clay in ratios of 1 and 2 phr exfoliated well in a matrix of PP blended with PP-g-MA, with an exception of agglomerate formation for 5 phr clay loading. The exfoliation of silicate layers was evaluated by TEM and Wide-angel X-ray scattering (WAXS). Clay dispersion increased the barrier properties by creation a tortuous path to limit the diffuse of oxygen molecules through the PP matrix. The 2 phr of clay provided improved resistance by increasing the oxygen barriers.

Girdthep *et al.* [29] studied the biodegradable nanocomposite films base on PLA containing silver-loaded kaolinite (AgKT). AgKT played a major role in enhancing the properties of compatibilized PLA/poly(butylene adipate-co-terph-thalate) (PBAT) blend including mechanical and thermal properties was increased due to AgKT fine caused efficient interaction between polymer matrix and the filler. Moisture barrier property was essentially improved owing to effective nucleation induced by AgKT. The nanocomposite film could storage dried longan shelf life of up to 308 days that may cover storage duration of other dried food products.

Espinosa *et al.* [30] studied the blown nanocomposite films from polypropylene and talc. The particle size and the amount of talc affect the distribution in the PP matrix. The talc particle distribution was arranged according to the flow direction of PP. The appropriate amount of talc was 1 and 3%, while 5% talc provided the agglomerate. Due to talc could be acting as nucleation agent, the mechanical and thermal properties of PP composites were increased. In addition, WVTR of polymer composite decreased as the

amount of talc was increased which was related to the amount of crystals increased. The results of tomato storage at 25 ℃ showed that PP composite films could maintain the weight loss of tomato better than PP film.

According to the previous researches, it was found that LDPE could enhance the flexibility and tear resistance of the blend, while PLA and clay could improve the oxygen permeability of composite film. Therefore, in this study, the PP, LDPE, PLA and clay composite film would be the new material with good stiffness, good strength, high tear resistance, good oxygen and water vapor barrier and biodegradable property. Moreover, the composite film could be applied for the single layer barrier film for food packaging.

CHAPTER III

METHODOLOGY

3.1 Materials

Polymer resins used in this research are presented in Table 3.1

Table 3.1 Materials and sources

Material	Grade	Density (g/cm^3)	Melt flow index 230 ºC/ 2.16 kg (g/10 min)	Source
Iso-polypropylene resin (PP)	1126NK	0.905	11	IRPC Public Company Limited, Thailand
Linear low density polyethylene resin (LDPE)	C510Y	0.921	12	PETRONAS Chemicals Group Berhad, Malaysia
Poly(lactic acid) (PLA)	4043D	1.24	13	Nature Work LLC, USA

Organoclay was Cloisite 20 supplied by BYK-Chemie GmbH, Germany. It is montmorillonite (MMT) treated with bis (hydrogenated tallow alkyl) dimethyl ammonium. The dry particle size is less than 10 µm. The density is 1.77 g/cm^3 and interlayer spacing of d_{001} is 3.16 nm.

Compatibilizer used was Polybond®3200, homopolymer polypropylene-graft-maleic anhydride (PP-g-MA) supplied by Addivant corporation, USA. The maleic anhydride content is in the range of 0.8 to 1.2 wt%.

3.2 Apparatus

Table 3.2 The list of major instruments used in the research

Instrument	Model	Manufacturer
Twin-screw extruder	ZSE 27 MAXX	Leistritz, Germany
Twin-screw extruder	ZK-25E	Dr. COLLIN, Germany
Melt flow indexer	MF50	CEAST, Italy
Differential Scanning Calorimeter	DSC 214 Polyma	NETZSCH, Germany
Thermogravimetric Analysis	TG 209F1 Libra	NETZSCH, Germany
Universal tensile tester	Instron 5566	Instron, USA
Transparency meter	BYK-Gardner haze gard plus	BYK-Gardner, Germany
Scanning Electron Microscope	SU3500	HITACHI, Japan
Transmission Electron Microscope	TECNAI 20	Phillips, Netherlands
X-ray diffractometer	TTRAX III	Rigaku, Japan
Oxygen Transmission Rate	OX-TRAN 2/21	Mocon, USA
Water Transmission Rate	7002	Illinoise, UK
Electronic weight balance	MS-70	AND, Japan

3.3 Experimental procedures

3.3.1 Preparation of compound

All components of polymer blends and polymer nanocomposite were mixed physically in a hi-speed mixer. Then, well-premixed materials were loaded into a Leistritz twin-screw extruder (D = 27 mm, L/D = 48) via a hopper (Figure 3.1). Twin screw extruder was operated at a rotational speed of 180 rpm. The temperature profiles of zone 1, zone 2, zone 3, zone 4, zone 5, zone 6, zone 7, zone 8, zone 9, zone 10, zone 11, and die were 170 ℃, 170 ℃, 180 ℃, 180 ℃, 190 ℃, 190 ℃, 195 ℃, 195 ℃, 200 ℃, 200 ℃, 205 ℃, and 205 ℃, respectively.

The compounding recipes of polymer blends and polymer nanocomposite are given in Table 3.3

Table 3.3 Recipes of polymer blends *a*nd polymer nanocomposite compound

Sample code* (PP/LDPE/PLA/MMT)	PP (%)	LDPE (%)	PLA (phr)	Montmorillonite (phr)	PP-g-MA (phr)
100/0/0/0	100	0	0	0	0
90/10/0/0	90	10	0	0	0
85/15/0/0	85	15	0	0	0
80/20/0/0	80	20	0	0	0
0/100/0/0	0	100	0	0	0
80/20/25/0	80	20	25	0	3
80/20/35/0	80	20	35	0	3
80/20/0/1	80	20	0	1	3
80/20/0/3	80	20	0	3	3
80/20/0/5	80	20	0	5	3
80/20/25/3	80	20	25	3	3
80/20/25/5	80	20	25	5	3

*a/b/c/d denoted the phr of PP, LDPE, PLA and MMT, respectively.

Figure 3.1 Twin Screw Extruder (ZSE 27 MAXX, Leistritz Germany).

3.3.2 Preparation of film

Polymer blend and polymer nanocomposite films were prepared using extrusion machine (ZK-25E, Dr. COLLIN) (Figure 3.2). The extruder temperature profile of zone 1, zone 2, zone 3, zone 4, zone 5, zone 6, zone 7, zone 8, zone 9, zone 10, zone 11, and die were 70 ℃, 110 ℃, 180 ℃, 180 ℃, 190 ℃, 190 ℃, 190 ℃, 200 ℃, 200 ℃, 200 ℃, 210 ℃, and 210 ℃, respectively. The screw rotation speed was 60 rpm. The chill roll temperature was 45 ℃ and the take-off speed was 0.45 m/min. The resultant film thickness was 70-75 μm. All films were stored in a controlled room before test.

Figure 3.2 Twin Screw Extruder (ZK-25E, Dr. COLLIN Germany).

3.3.3 Characterization

i) Mechanical properties

The tensile test was performed to determine the elastic modulus, tensile strength, and elongation at break using the universal testing machine (Instron 5566, USA) (Figure 3.4) with a load cell of 500 N, at a crosshead speed of 50 mm/min and gauge length of 50 mm, according to ASTM D882. Each formulation film was prepared with dimension 100 x 25 x 0.070 mm for the test in the machine direction (MD) and transverses direction (TD) and the average values of five measurements were reported.

The film trouser tear test was performed using the universal testing machine (Instron 5566, USA), with constant crosshead speed of 300 mm/min and a gap between grips of 50 mm. At least 5 specimens of all film formulations, for each studied direction (MD and TD), were assayed at room temperature recording the corresponding

load-time curves. According to ASTM D1938 standard test method, samples (25 x 10 mm) with a slit at 12.5 mm were prepared (Figure 3.3).
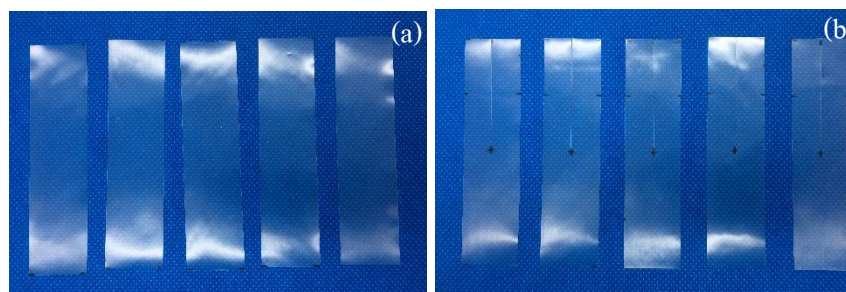
Figure 3.3 Film sample (a) Tensile strength test and (b) Tear strength test.

Figure 3.4 Universal testing machine (Instron 5566, USA).

ii) Thermal properties

The thermal properties of polymer samples were determined in terms of the melting temperature (T_m), the crystallization temperature (T_c) by differential scanning calorimeter (DSC) 214 Polyma (NETZSCH, Germany) in the temperature range of 30-300 ºC under nitrogen atmosphere. About 5-10 mg samples were tested at the same heating and cooling rate of 10 ºC/min in three consecutive scans: heating, cooling and heating.

The thermal stability of PP/LDPE blends, PP/LDPE/PLA blends, and polymer nanocomposite were characterized by a thermogravimetric analyzer (TG 209F1

Libra, NETZSCH Germany). About 25 mg of sample was heated from 25 to 600 ºC at heating rate 20 ºC/min under nitrogen atmosphere with a gas flow rate of 20 ml/min.

iii) Optical property

The transparency of film samples with average thickness of 70 μm was measureed in percent haze by BYK-Gardner haze gard plus instrument (BYK-Gardner, Germany) (Figure 3.5). The presented results are the averages of five tests per sample.

Figure 3.5 BYK-Gardner haze gard plus instrument (BYK-Gardner, Germany).

iv) Morphology

Scanning electron microscope (SEM, SU3500, HITACHI Japan) (Figure 3.6) was used to characterized the morphology of PP/LDPE/PLA blends. The sample coated with gold to prevent charging were examined under SEM observation. And the element mapping was analyzed by scanning electron microscopy-energy dispersive X-ray spectrometry (SEM-EDS) to provide oxygen mapping and their distribution in polymer matrix.

Figure 3.6 Scanning electron microscope (SU3500, HITACHI Japan).

The dispersion quality of the nanoparticles within the matrix and the nanostructure of the nanocomposites were investigated using transmission electron microscope (TECNAI 20 Phillips, Netherlands) (Figure 3.7), operated at 100 kV.

Figure 3.7 Transmission electron microscope (TECNAI 20 Phillips, Netherlands).

v) X-ray diffraction (XRD)

X-ray diffraction measurement was made directly from organoclay powder, and nanocomposite films. The test was performed using the X-ray diffractometer (TTRAX III, Rigaku Japan) with CuK_α radiation (λ = 0.15406 nm) operated at 50 kV and 300 mA. The diffraction curves were obtained from 1 to 10º at a scanning rate of 1º min^{-1}.

$$d_{hkl} = \frac{\lambda}{2sin\theta}$$ (3.1)

where   d is the lattice spacing, λ is the wavelength of incident light, and θ is the angle of incidence

vi) Permeability properties

The permeability to oxygen of polymer blends and composite films were measured using an oxygen permeation analyzer (OX-TRAN 2/21 Module MT, Mocon USA), according to ASTM D3985. The test condition is 23 ºC and 0% RH.

The permeability of water vapor of polymer blends and composite films were measured using a water vapor permeation analyzer (7002, Illinois UK) at 37.8 ºC, and 90% RH according to ASTM F1249.

3.3.4 Biodegradation

PP, LDPE, PP/LDPE/PLA/MMT, and the commercial film were prepared as same as section 3.3.3: *i*. The specimen weight was measured using a laboratory electronic weight balance (MS-70, AND Japan) and buried at 15 cm below the surface of natural soil from February to April 2019 at the temperature of 34 ºC and 90% RH. At the desired time (15, 30, 60 and 90 day after burial), the buried specimens were removed from the soil to weigh and test for their tensile strength (ASTM D882).

$$Weight\ loss\ (\%) = (\frac{W_1 - W_2}{W_1}) \times 100 \qquad (3.2)$$

where W_1 and W_2 are the weight before and after burial test

3.3.5 Packaging condition and storage

In order to provide a very cost-efficient alternative to overcome barrier deficiencies of traditional food packaging. Tomatoes, sorted for uniform size were packaged in PP, 80/20/25/3 and the commercial films (Figure 3.8). The packaging containing tomatoes were stored under controlled conditions of temperature (14-20 ºC). Control samples were kept unsealed under similar environmental condition of temperature and RH. The weight of each tomato was measured using a laboratory electronic weight balance (MS-70, Japan). The physiological weight loss was calculated and expressed in percentage base on initial weight of samples.

| Control | PP film | 80/20/25/3 film | Commercial film |

Figure 3.8 The tomato package using various films

CHAPTER IV

RESULTS AND DISCUSSION

4.1 Effect of blend ratio on the mechanical, thermal and optical properties of PP/LDPE/PLA blends

4.1.1 Mechanical properties

The mechanical properties in terms of tensile properties and tear strength of blend films in machine direction (MD) and transverse direction (TD) are presented in Table 4.1 and Figure 4.1a-d. From the Figure 4.1a, the MD tensile strength of PP/LDPE blend films did not show the significant change with the addition of 10-15 wt% LDPE (from 34.0 MPa for neat PP to 34.2 and 34.8 MPa for 10 and 15 wt% LDPE, respectively). This implied that the stress was effectively transferred from the major PP matrix to the greatly dispersed LDPE. While the tensile strength of PP/LDPE blends was slightly decreased with the increase of LDPE content up to 20 wt% (32.5 MPa) due to the low tensile strength of LDPE in PP matrix [2]. Therefore, the 80/20 PP/LDPE was selected for further study on the effect of PLA content.

For PP/LDPE/PLA blend films, the tensile strength of 80/20/25 PP/LDPE/PLA slightly increased (34.5 MPA), whereas 80/20/35 PP/LDPE/PLA blend was decreased (24.5 MPa). This indicated that the mechanical properties of blend depended on the compatibility of components. The interaction of PLA with PP/ LDPE matrix became weaker when the PLA content increased [4].

The TD tensile strength was lower than that in MD because of the higher oriented polymer chain in MD. The TD tensile strength was decreased with increasing LDPE and PLA contents increasing. The TD tensile strength of 80/20 PP/LDPE was decreased to 20.0 MPa compared with PP (27.4 MPa) because the LDPE with branch macromolecules provided the entanglement and amorphous phase in the PP matrix [31]. Moreover, the tensile strength of PP/LDPE/PLA was decreased from 20.0 MPa for 80/20/0 to 12.7 and 9.6 MPa for 80/20/25, 80/20/35, respectively, because PLA chain

oriented along in the MD and acted as stress concentration point leading to crazes at the interphase during extend extrusion.

The elongation of polymer blends was compared in Figure 4.1b. The MD elongation at break was slightly increased with increasing LDPE (from 400% for PP neat to 480-490% for PP/LDPE blend with 10-20wt%). This behavior ascribed to the reason was the phase separation of LDPE in the PP phase resulting the inhibition of PP crystallization. Thus, the PP/LDPE blends were more ductility than PP neat. While, adding PLA adding provided the decreased MD elongation at break (from 480% for 80/20/0/0 to 340 and 220 % for 80/20/25, 80/20/35, respectively) due to intrinsically low elongation at break value of PLA with hard and brittle properties. The TD elongation at break value was decreased with increasing LDPE content (from 420% for PP neat to 320% for 20 wt% of LDPE adding) because the branch macromolecules of LDPE provided entanglements during extension process. In addition, PLA addition greatly affected the TD elongation at break (from 320% of 80/20/0 to 1.86 and 1.14% for 80/20/25 and 80/20/35, respectively) due to the easily craze at the interphase and the brittle property of PLA [4].

From the Figure 4.1c, Both MD and TD tensile modulus were decreased with increasing LDPE content because the low tensile modulus of LDPE introduced softness of PP/LDPE blend [26]. However, MD and TD tensile modulus of PP/LDPE/PLA were increased blend with increasing PLA content

From the Figure 4.1d, The tear strength in TD was higher than that in MD of film because the orientation of the molecules in MD resulting the lamella grown in TD [31]. The MD tear strength of PP/LDPE and PP/LDPE/PLA blend films was lower than that of PP films. Increasing LDPE and PLA content reduced tear strength because of the phase inconsistency from phase separating morphology of PP, LDPE and PLA. Moreover, the tear strength of PP/LDPE/PLA blend was decreased with PLA addition due to the brittle property of PLA (from 10.7 kgf/cm of 80/20/0 to 0.96 kgf/cm of 80/20/35). The TD tear strength of PP/LDPE blends was slightly increased with LDPE addition (from 43.9 kgf/cm of neat PP to 47.0 kgf/cm of 15 wt% LDPE), indicating that the toughness properties of

LDPE could improve the tear resistance of blend polymer. For the TD tear strength of PP/LDPE/PLA blend films, the result of PLA addition could not be verified by trouser tear analysis because the samples were easily teared in MD during testing.

Table 4.1 Effect of blend ratio on mechanical properties of PP/LDPE/PLA blend films

Sample code*	Tensile strength (MPa)		Elongation at break (%)		Tensile modulus (MPa)		Tear strength (kgf/cm)	
	MD	TD	MD	TD	MD	TD	MD	TD
100/0/0	34.0±1.0	27.4±1.0	400±19	420±11	1068±32	983±33	17.8±1.4	43.9±3.1
90/10/0	34.2±1.4	23.0±1.1	480±18	390±9	980±26	907±26	16.6±2.1	38.1±0.6
85/15/0	34.8±0.7	21.2±0.8	490±27	350±17	952±31	881±32	11.7±1.2	47.0±1.2
80/20/0	32.5±1.4	20.0±1.1	480±5	320±18	948±18	862±33	10.7±0.3	44.8±0.3
0/100/0	13.8±0.5	7.9±1.5	150±8	290±34	139±7	131±5	27.6±0.9	42.2±0.5
80/20/25	34.5±0.3	12.7±0.7	340±13	1.86±0.2	1557±64	1080±15	1.38±0.1	23.3±1.4
80/20/35	24.5±0.8	9.96±1.2	220±5	1.14±0.2	1737±45	1226±49	0.96±0.1	11.5±1.3

*a/b/c denoted the phr of PP, LDPE and PLA, respectively.
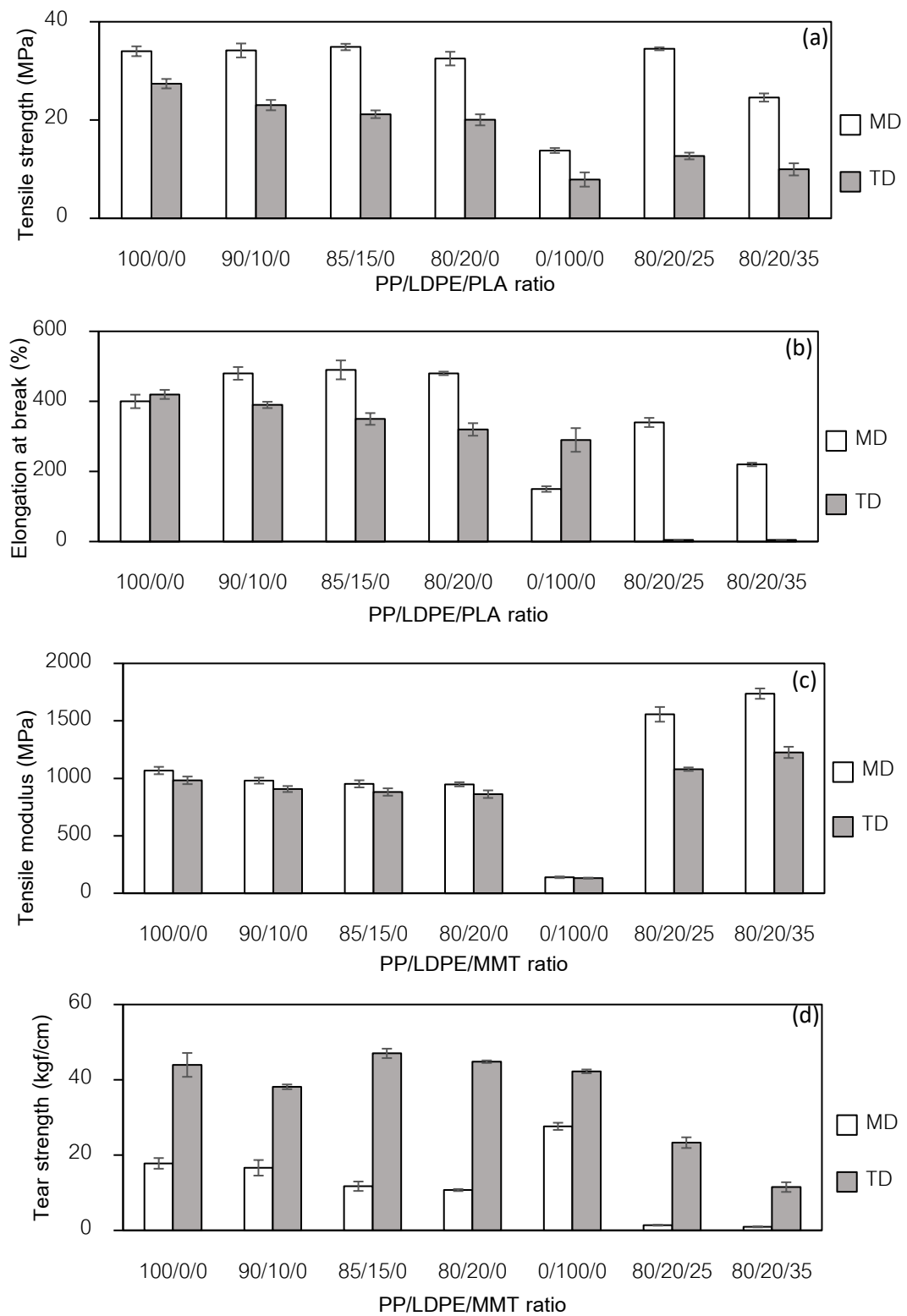
Figure 4.1 Effect of blend ratio on mechanical properties of blend films: (a) Tensile strength, (b) Elongation at break, (c) Tensile modulus and (d) Tear strength.

4.1.2 Thermal properties

The thermal properties of blends were determined by DSC and the thermal stability was characterized by TGA. DSC analysis of blends in terms of melting temperature (T_m), crystallization temperature (T_c), enthalpy of melting (ΔH_m), enthalpy of crystallization (ΔH_c) and %crystallinity is presented in Table 4.2. The T_m of PP, LDPE and PLA was 165.9, 108.8 and 154.2 ºC, respectively. The PP/LDPE blends at ratio of 90/10, 85/15 and 80/20 displayed two melting peaks associated with the melting of PP and LDPE. The PP/LDPE/PLA blends displayed three melting peaks of PP, LDPE and PLA (Figure 4.2a), indicating the thermodynamically immiscibility [2]. The melting peak positions of the components in blends remain unchanged relative with the pristine polymers. The ΔH_m of PP/LDPE blend (peak intensity) reduced with increasing LDPE content (from 104.6 J/g of neat PP to 62.8 J/g of 80/20 blend). The %crystallinity of PP in blends was decreased with increasing LDPE and PLA content (from 50.5% of neat PP to 30.3% for 80/20 PP/LDPE and 31.7% of 80/20/35 PP/LDPE/PLA blend) due to the LDPE and PLA inhibited the crystallization of PP and decreasing PP content in blends. The T_c of PP and LDPE was 110.1 ºC and 91.5 ºC, respectively, while T_c of PLA could be observed because there was no enough time to crystallize PLA within the cooling time frame [32] (Figure 4.2b). From table 4.5, T_c of PP remained not change in the range of 110.8-112.1 ºC, this implied that LDPE and PLA addition did not affect the crystallization temperature. However, ΔH_c of PP in blends was decreased with increasing PLA content (from 71.3 J/g of 80/20/0 blend to 59.27 and 52.59 J/g of 80/20/25 and 80/20/35 blends, respectively). This postulated that the PLA in PP matrix make the PP chain packed difficultly, since the presence of PLA acted an impurity that caused the decrease in crystallinity [33].

The TGA analysis of blends are shown in Table 4.3 and Figure 4.3a-b. The TGA curve of pure polymer and PP/LDPE blends exhibited the single step decomposition process (Figure 4.3a). From the Table 4.3, PP and PP/LDPE blends started to decompose at above 432 ºC, while LDPE started to decompose at 452 ºC. PP had lower decomposition temperature than LDPE because the tertiary carbon in PP backbone was

easily attacked compared with LDPE [2]. It can be seen that the decomposition temperature of 80/20 PP/LDPE blends tended to be increased (from 432 ºC of neat PP to 434.4 ºC of 80/20 blend). However, the PP/LDPE/PLA blends had two-step degradation process, the first one indicating PLA decomposition and the second one at higher temperatures, relating to PP and LDPE degradation (Figure 4.3b). The thermal stability of PLA was lower than that of 80/20 PP/LDPE blend, which T_{onset} of PLA and 80/20 PP/LDPE blend was 350.7 and 457.5 ºC, respectively. The percentage weight loss in the first and second decomposition steps was related to the amount of PLA and PP. The incorporation of PLA in PP/LDPE blend led to the shift of onset degradation temperature to lower values and the T_{onset} of PLA was decreased from 350.7 ºC to 329.4 and 330.6 ºC of 80/20/25 and 80/20/35, respectively. Moreover, the T_{onset} of PP in blends was decreased from 457.5 to 395.2 and 397.6 ºC of 80/20/25 and 80/20/35, respectively, implying that blending of PLA in PP and LDPE reduced the thermal stability and thermal sensitivity.

Table 4.2 Effect of blend ratio on the thermal properties of PP/LDPE/PLA blends

Sample code*	$T_{m,PP}$ (ºC)	$T_{m,LDPE}$ (ºC)	$T_{m,PLA}$ (ºC)	$T_{c,PP}$ (ºC)	$T_{c,LDPE}$ (ºC)	$\Delta H_{m,PP}$ (J/g)	$\Delta H_{m,LDPE}$ (J/g)	$\Delta H_{c,PP}$ (J/g)	$\Delta H_{c,LDPE}$ (J/g)	%crystallinity of PP (%)
100/0/0	165.9	-	-	110.1	-	104.6	-	99.0	-	50.5
90/10/0	165.2	106.8	-	110.8	95.3	80.1	3.55	78.9	1.19	38.7
85/15/0	164.8	107.0	-	110.7	95.1	72.9	7.33	74.8	4.83	35.2
80/20/0	164.7	107.3	-	110.8	94.5	62.8	11.9	71.3	9.12	30.3
0/100/0	-	108.8	-	-	91.5	-	106.1	-	74.7	-
80/20/25	163.6	107.1	151.7	112.1	94.2	65.24	4.21	59.27	7.38	31.5
80/20/35	163.1	107.0	152.1	111.9	94.6	65.61	6.87	52.59	6.21	31.7
0/0/100	-	-	152.4	-	-	-	-	-	-	-

*a/b/c denoted the phr of PP, LDPE and PLA, respectively.
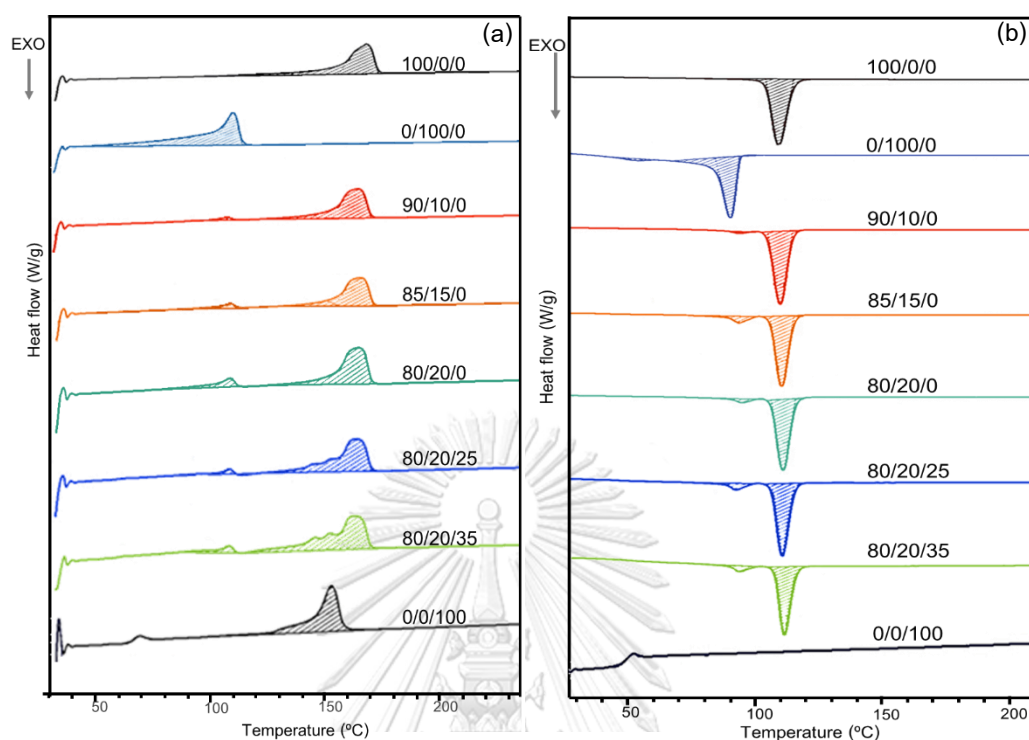
Figure 4.2 DSC curves of PP/LDPE/PLA blends: (a) DSC heating curve (b) DSC cooling curve.

Table 4.3 Effect of blend ratios on thermal stability of PP/LDPE/PLA blends

Sample code*	T_{onset1} (°C)	T_{onset2} (°C)	$T_{50\%}$ (°C)	$T_{end\ set}$ (°C)	Mass change (%)		Residue (%)
					Step 1	Step 2	
100/0/0	432.0	-	456.9	481.7	100	-	-
90/10/0	432.3	-	456.0	479.6	100	-	-
85/15/0	432.3	-	456.4	479.4	100	-	-
80/20/0	434.4	-	457.5	480.3	100	-	-
0/100/0	452.8	-	473.3	493.1	100	-	-
80/20/25	329.4	395.2	-	457.1	34.94	65.1	-
80/20/35	330.6	397.6	-	468.8	40.8	59.2	-
0/0/100	350.7	-	380.6	400.3	100	-	-

*a/b/c denoted the phr of PP, LDPE and PLA respectively.
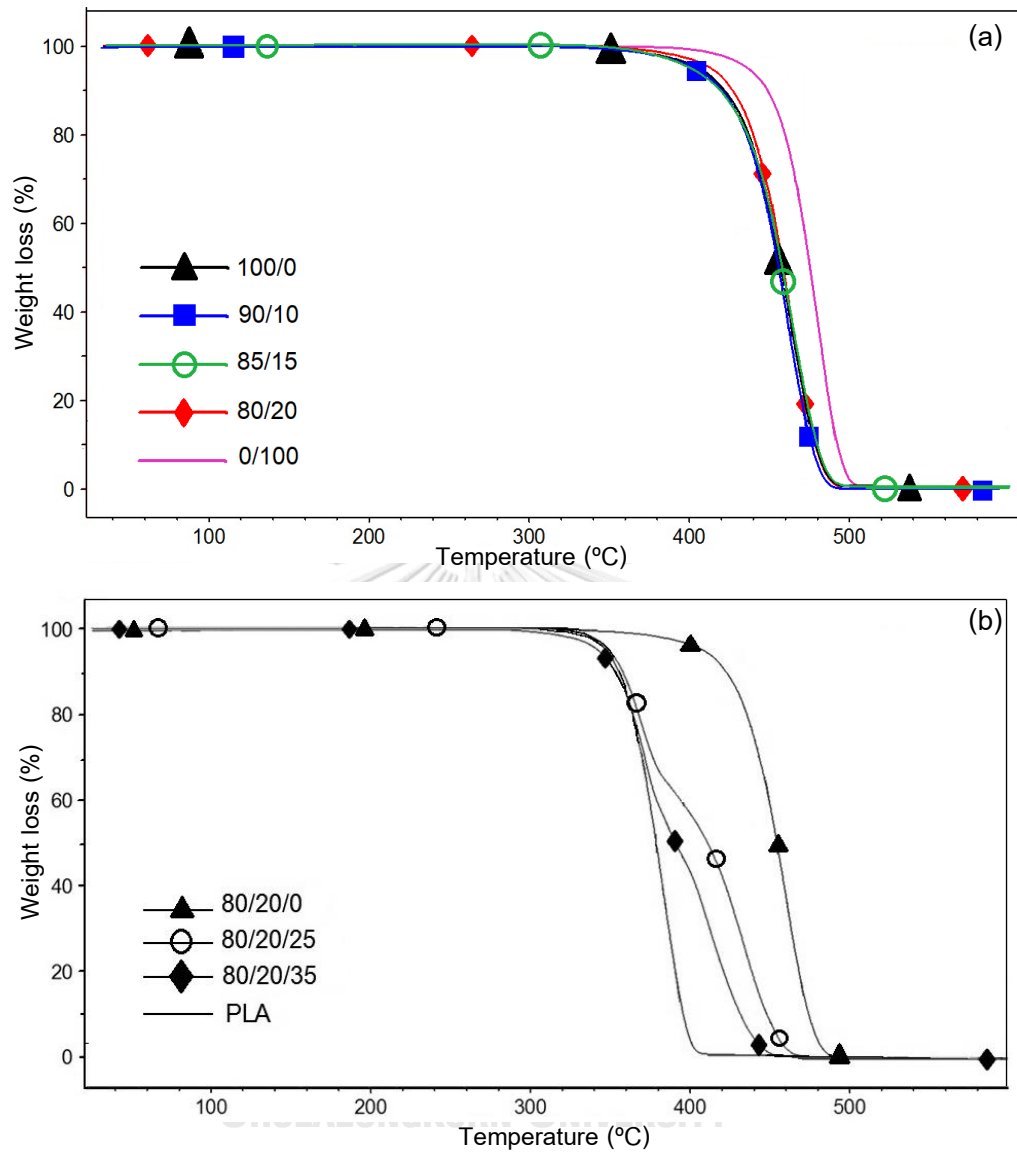
Figure 4.3 TGA curves of blends: (a) PP/LDPE blends (b) PP/LDPE/PLA blends.

4.1.3 Optical property

The optical property of blends was determined in terms of a haze value as presented in Table 4.4. The haze value of samples was increased with increasing LDPE and PLA contents (from 16.4% of neat PP to 20.2-22.3% of PP/LDPE blends and 57.9-64.8% of PP/LDPE/PLA blends). These results indicated that the transparency of PP/LDPE/PLA blend films was reduced due to the immiscible blend system. The PP/LDPE/PLA blend was hazier than PP/LDPE blend due to incompatibility of PLA and PP. The blend films exhibited translucent, that the covering objects could be seen well (Figure 4.4), 80/20/35 PP/LDPE/PLA provided the worse mechanical and optical properties. Therefore, 80/20/25 PP/LDPE/PLA blend film was the appropriate ratio to be selected for further study on the effect of MMT content.

Table 4.4 Effect of blend ration on the optical property of PP/LDPE/PLA blend film

Sample code*	Haze (%)
100/0/0	16.4
90/10/0	20.2
85/15/0	20.9
80/20/0	22.3
80/20/25	57.9
80/20/35	64.8

*a/b/c denoted the phr of PP, LDPE and PLA respectively.
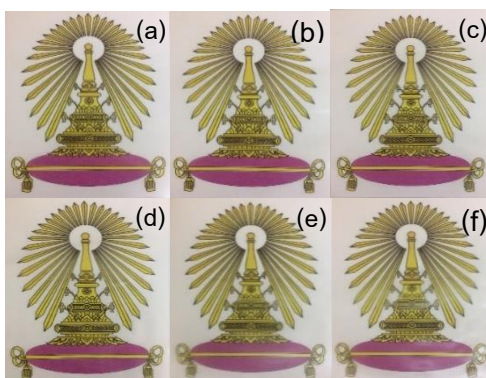
Figure 4.5 Effect of blend ratios on optical property: (a) 100/0/0, (b) 90/10/0,
(c) 85/15/0, (d) 80/20/0, (e) 80/20/25 and (f) 80/20/35.

4.2 Effect of MMT loading on properties of PP/LDPE/PLA/MMT composite film

4.2.1 Mechanical properties

The tensile properties and tear strength of PP/LDPE/PLA/MMT composite films are summarized in Table 4.5. From Figure 4.5a, the MD tensile strength was decreased with increasing MMT content (from 32.5 MPa of 80/20/0/0 to 28.7 MPa of 80/20/0/5 and from 34.5 MPa of 80/20/25/0 to 21.6 MPa of 80/20/25/5) . This result is a consequence of restriction of polymer chain movement by the filler existence [4]. The TD tensile strength of PP/LDPE/MMT composite films exhibited no significant change with increasing MMT content but the TD tensile strength of PP/LPDE/PLA/MMT composite films was increased (from 12.7 MPa of 80/20/25/0 to 15.6 MPa of 80/20/25/5) indicating that MMT could improve the compatibility between PP and PLA due to the hydrophilicity of organic compound treated on clay surface and the hydrophobic clay layer [29].

From the Figure 4.5b, the MD elongation at break of composite films was slightly decreased with increasing MMT content inferred that the nanocomposite restriction of the polymer chain movement and the stress point at the nanoparticle leading to the progress of crazes at the interphase. However, TD elongation at break of 80/20/0/1 and 80/20/0/3 PP/LDPE/PLA/MMT films was higher than 80/20/0/0 film because MMT provided the crystal orientation in MD rather than TD during process. Thus, the increasing amorphous phase occurred in TD resulting the increased TD elongation at break. While, the TD elongation at break of 80/20/0/5 film was decreased due to the agglomeration of MMT causing the disruption of interfacial adhesion between MMT and polymer. Considering the PP/LDPE/PLA/MMT composite film, TD elongation at break was increased with increasing the MMT content (from 1.86% of 80/20/25/0 to 12% of 80/20/25/5) implying that MMT improved the interfacial adhesion between PP and PLA.

From Figure 4.5c, the tensile modulus of composite films was increased with increasing MMT content both MD and TD because MMT provided the nucleation leading to the formation of smaller sized PP crystals [29], that increased the stiffness. Moreover, the higher stiffness of MMT compared with PP could govern the modulus increment on nanocomposite films.

The tear strength of composite films is shown in Figure 4.5d. For the PP/LDPE/MMT composite films, the MD tear strength was decreased with increasing MMT content due to that MMT provided the orientation of the macromolecule in the machine direction. In consequence, the amount of grown lamella increased in transverse direction [30], resulting the increased TD tear strength (from 44.8 kgf/cm of 80/20/0/0 to 68.0 kgf/cm of 80/20/0/5). For the PP/LDPE/PLA/MMT composite films, both MD and TD tear strengths were increased with MMT addition (from 1.38 kgf/cm of 80/20/25/0 to 6.06 kgf/cm of 80/20/25/5). This result indicated that MMT could improve the compatibility between PP and PLA.

Table 4.5 Effect of MMT loading on mechanical properties of PP/LDPE/PLA/MMT composite film

Sample code*	Tensile Strength (MPa)		Elongation at break (%)		Tensile modulus (MPa)		Tear strength (kgf/cm)	
	MD	TD	MD	TD	MD	TD	MD	TD
80/20/0/0	32.5±1.4	20.0±1.1	480±5	320±18	948±18	862±33	10.7±0.3	44.8±0.3
80/20/0/1	32.9±2.0	21.7±1.2	470±24	390±12	1348±54	954.±36	16.0±1.9	66.9±4.4
80/20/0/3	31.3±1.7	20.8±1.0	460±25	360±5	1355±70	1138±119	5.30±0.7	69.2±0.7
80/20/0/5	28.7±1.7	18.9±0.9	440±27	330±13	1231±39	1111±32	4.82±0.2	68.0±4.2
80/20/25/0	34.5±0.3	12.7±0.7	340±13	1.86±0.2	1557±64	1080±15	1.38±0.1	23.3±1.4
80/20/25/3	23.9±0.5	14.9±0.8	380±5	11±2	1890±87	1598±106	6.08±0.7	68.3±2.4
80/20/25/5	21.6±0.8	15.6±0.2	350±14	12±1	1910±42	1676±79	6.06±0.3	70.0±1.6

*a/b/c/d denoted the phr of PP, LDPE, PLA and MMT, respectively.
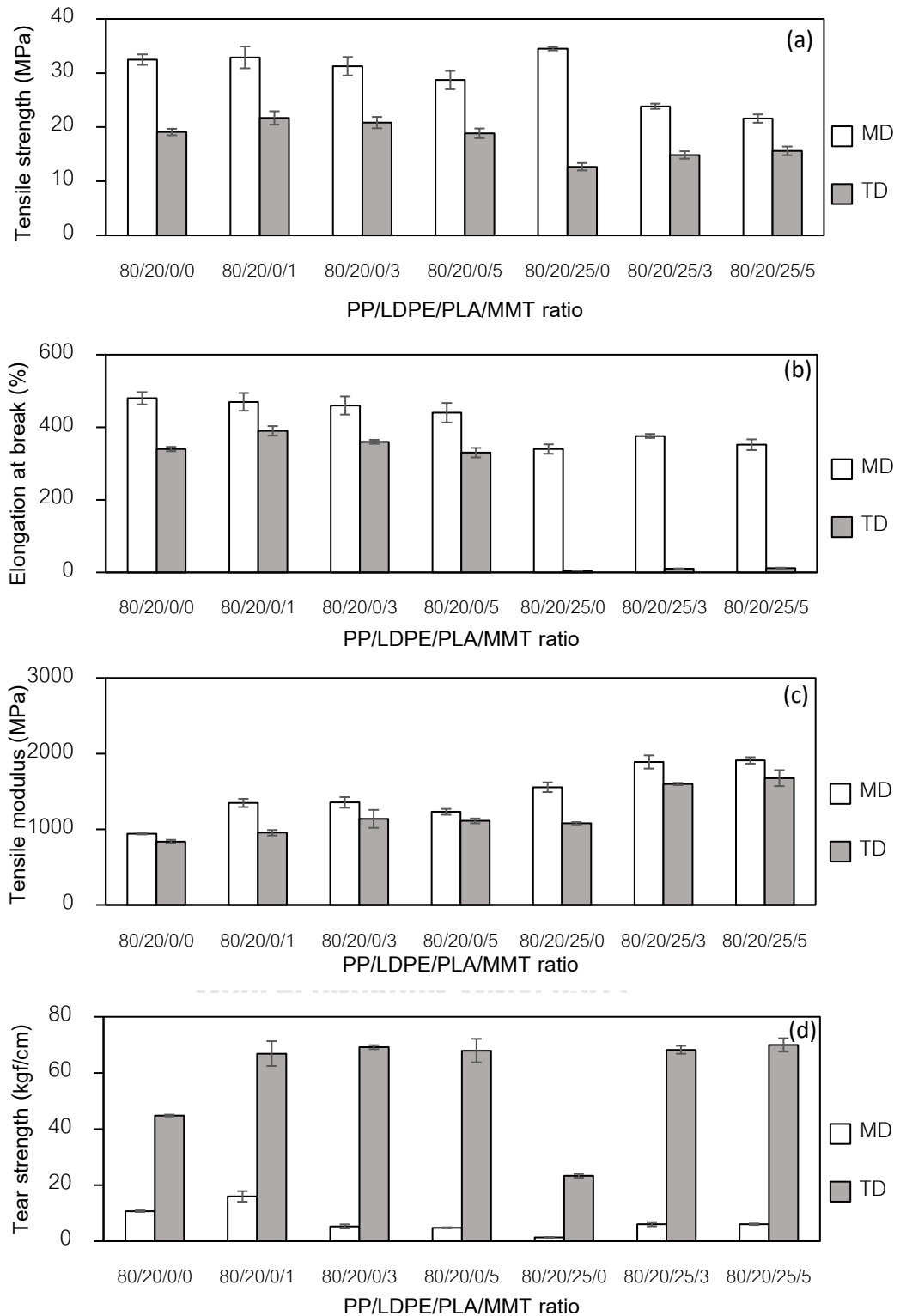
Figure 4.6 Effect of blend ratio on mechanical properties of PP/LDPE/PLA/MMT composite films: (a) Tensile strength, (b) Elongation at break, (c) Tensile modulus and (d) Tear strength.

4.2.2 Thermal properties

The thermal behavior of the polymer composites was evaluated by DSC (Table 4.6 and Figure 4.6a-b) and the thermal stability was determined by TGA as seen in Table 4.7 and Figure 4.7a-b. From Figure 4.7a-b, the melting peak positions of the blends remained unchanged relative to the pristine polymers. From Table 4.7, $T_{c,PP}$ of PP/LDPE/MMT composites was increased with increasing MMT content (from 110.8 °C of 80/20 PP/LDPE blend to 116.2-116.7 °C of 80/20/3 and 80/20/5 PP/LDPE/MMT). This behavior was due to the increment of MMT particle concentration that could act as the nucleating agent. It can be seen that the melting and crystallization enthalpy of PP ($\Delta H_{m,PP}$, $\Delta H_{c,PP}$) shown an increased by MMT addition. Thus, MMT induced the crystallinity degree of film (from 30.3% of 80/20 PP/LDPE blend to 33.5% of 80/20/5 PP/LDPE/MMT). However, the MMT addition increased only the $\Delta H_{m,PP}$ but did not affect the $T_{c,PP}$ and $\Delta H_{c,PP}$ of PP/LDPE/PLA/MMT composite films because PLA in PP matrix made the PP chain packe difficulty.

The thermal stability of the polymer composites evaluated by TGA is presented in Table 4.7. All PP/LDPE/MMT composites exhibited a single step degradation (Figure 4.7a). The thermal degradation of the PP/LDPE blends started at 434 °C and increased with MMT addition (450.3-454.3 °C). In contrast, PP/LDPE/PLA/MMT composite at 80/20/25/3 and 80/20/25/5 ratios also had a two-step degradation process similar to 80/20/25/0 PP/LDPE/PLA (Figure 4.7b). Thus, MMT addition affected the degradation temperature by first step increased $T_{onset,1}$ from 329.4 °C of 80/20/25/0 to 340.1 and 341.6 °C of PP/LDPE/PLA with 3 and 5 phr, respectively, and second step increased $T_{onset,2}$ from 395.2 °C of 80/20/25/0 to 439.7 and 442.3 °C of PP/LDPE/PLA with 3 and 5 phr, respectively. Therefore, MMT presence offered the higher stability of polymer composite than polymer blend films. This implied that MMT increased the crystallization and acted as a mass-transport barrier for the volatile products generated during thermal decomposition [29].

Table 4.6 Effect of MMT loading on thermal properties of PP/LDPE/PLA/MMT composite films

Sample code*	$T_{m,PP}$ (°C)	$T_{m,LDPE}$ (°C)	$T_{m,PLA}$ (°C)	$T_{c,PP}$ (°C)	$T_{c,LDPE}$ (°C)	$\Delta H_{m,PP}$ (J/g)	$\Delta H_{m,LDPE}$ (J/g)	$\Delta H_{c,PP}$ (J/g)	$\Delta H_{c,LDPE}$ (J/g)	%crystallinity of PP (%)
80/20/0/0	164.7	107.3	-	110.8	94.5	62.8	11.9	71.3	9.12	30.3
80/20/0/1	163.7	107.5	-	116.2	94.3	63.1	8.14	76.2	8.24	30.4
80/20/0/3	164.6	107.5	-	116.7	93.9	66.5	10.4	73.4	6.91	32.9
80/20/0/5	166.0	107.8	-	116.3	93,5	69.3	10.6	74.6	7.82	33.5
80/20/25/0	163.6	107.1	151.7	112.1	94.2	65.2	4.21	59.3	7.38	31.5
80/20/25/3	163.8	107.1	146.4	111.6	93.8	69.6	17.6	57.2	6.80	33.6
80/20/25/5	165.2	107.8	146.5	111.3	93.5	67.2	12.7	58.1	5.80	32.4

*a/b/c/d denoted the phr of PP, LDPE, PLA and MMT, respectively.
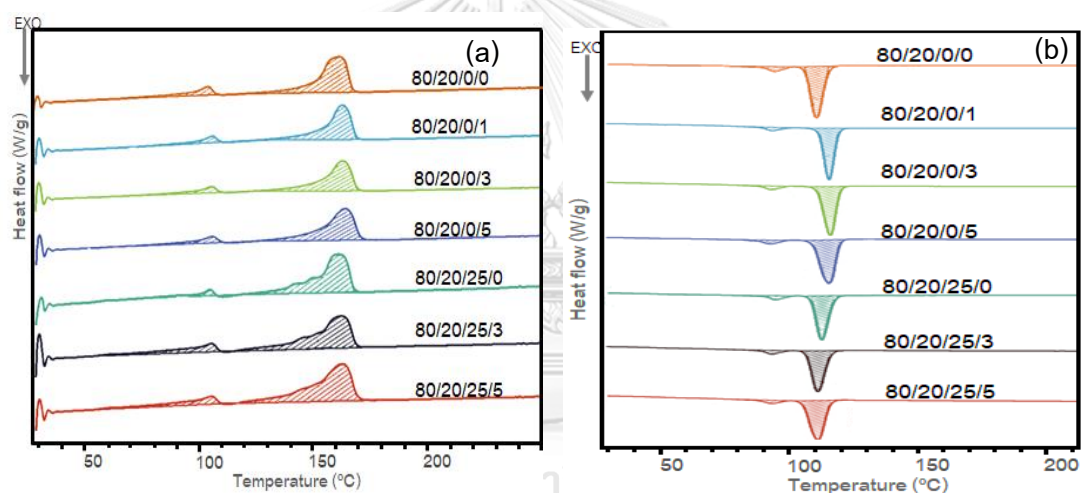
Figure 4.7 DSC curves of PP/LDPE/PLA/MMT composites: (a) DSC heating curve (b) DSC cooling curve.

Table 4.7 Effect of MMT loading on thermal stability of PP/LDPE/PLA/MMT composites

PP/LDPE/PLA/MMT*	$T_{onset,1}$ (°C)	$T_{onset,2}$ (°C)	$T_{50\%}$ (°C)	$T_{end\ set}$ (°C)	Mass change (%)		Residue (%)
					Step 1	Step 2	
80/20/0/0	434.4	-	457.5	480.3	100	-	0
80/20/0/1	450.7	-	459.6	468.2	98.9	-	1.05
80/20/0/3	450.3	-	460.9	468.2	97.9	-	2.06
80/20/0/5	454.3	-	462.2	470.0	95.5	-	4.46
80/20/25/0	329.4	395.2	-	457.1	41.8	58.2	0
80/20/25/3	340.1	439.7	-	465.9	19.4	74.9	0.19
80/20/25/5	341.6	442.3	-	460.7	17.2	70.7	3.22

*a/b/c/d denoted the phr of PP, LDPE, PLA and MMT, respectively.
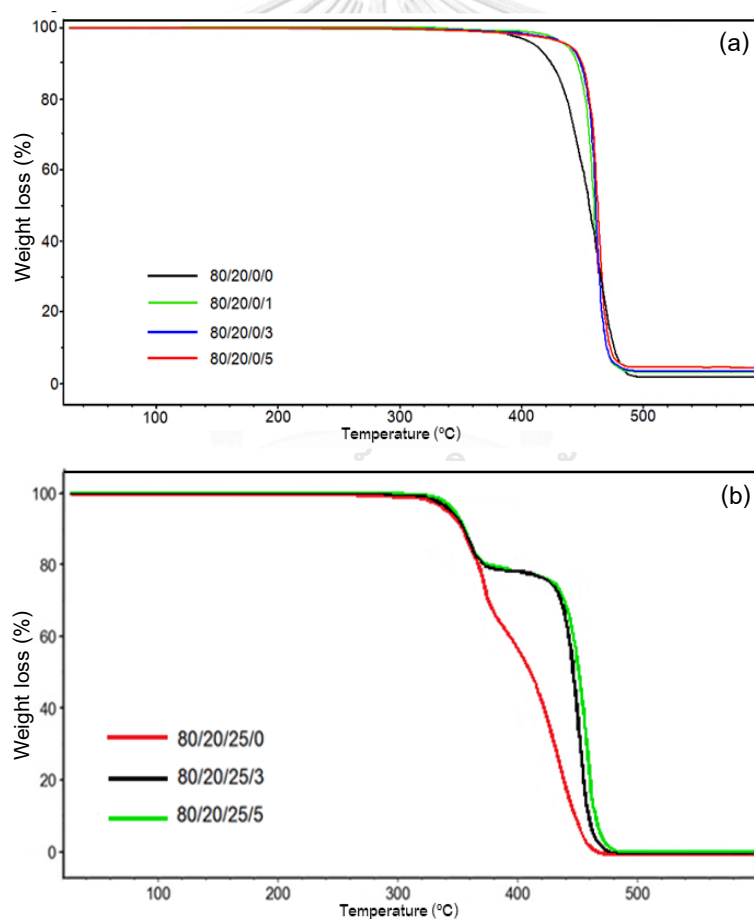
Figure 4.8 TGA curves of composites: (a) PP/LDPE/MMT composites

(b) PP/LDPE/PLA/MMT composites.

4.2.3 Optical property

The haze value of composite films is presented in Table 4.8. The haze value of PP/LDPE/MMT film with 1, 3 and 5 phr MMT exhibited no significant (22.3-23.1%). The haze value of 80/20/25/0 and 80/20/25/3 PP/LDPE/PLA/MMT film (56.4-54.7%) was higher than that of 80/20/0/0 and 80/20/0/3 due to the incompatibility of PLA. This result can also be explained that the particle size of MMT was smaller size than wavelength of visible light and good dispersion of MMT that provided the low light scattering. While the haze value of 80/20/25 PP/LDPE/PLA with 5 phr of MMT addition was slightly increased because the MMT particles were possibly aggregated leading to light scattering [30].

Table 4.8 Effect of MMT loading on optical property of PP/LDPE/PLA/MMT composite films

PP/LDPE/PLA/MMT*	Haze (%)
80/20/0/0	22.3
80/20/0/1	22.1
80/20/0/3	22.9
80/20/0/5	23.1
80/20/25/0	56.4
80/20/25/3	54.7
80/20/25/5	64.8

*a/b/c/d denoted the phr of PP, LDPE, PLA and MMT, respectively.
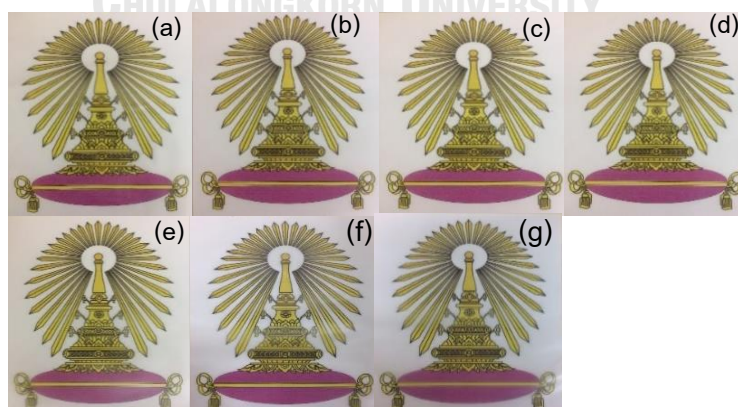
Figure 4.9 Effect of blend ratio on optical property: (a) 80/20/0/0, (b) 80/20/0/1, (c) 80/20/0/3, (d) 80/20/0/5, (e) 80/20/25/0, (f) 80/20/25/3 and (g) 80/20/25/5.

4.2.4 X-ray Diffraction

The effect of MMT loading on XRD patterns of composite films are shown in Figure 4.9. The calculated d_{001}-spacings are reported in Table 4.9. The position of (001) diffraction peak of Cloisite appeared at 2.73º and the calculated d_{001}-spacing was 3.23 nm. The (001) diffraction peak of PP/LDPE/MMT composite films shifted to the lower diffraction and the interlayer spacing of nanocomposite was higher than that of Closite. This implied that the polymer chain could move through the gallery in the layered clay and led to the intercalation and exfoliation formation.

The (001) diffraction peaks of PP/LDPE/MMT composite films shifted to higher diffraction angle with increasing MMT content. The interlayer spacing of nanocomposites was decreased from 4.33 nm of 80/20/1 to 3.65 and 3.53 nm 80/20/0/3 and 80/20/0/5, respectively. This result can be explained that the agglomeration of clay at higher content caused polymer molecule to diffused difficultly into the interlayer of agglomerated clay [34].

In contrast, the (001) diffraction peaks of PP/LDPE/PLA/MMT composite films shifted to the lower diffraction angle compared with PP/LDPE/MMT. The 80/20/25/3 and 80/20/25/5 composites had the interlayer spacing of 3.99 and 3.69 nm, respectively, that was larger than 80/20/0/3 and 80/20/0/5 composite with 3.65 and 3.53 nm. This demonstrated that adding PLA had the role in the increased interlayer spacing. The polar structure of PLA was more compatible with the polar structure of MMT than PP and LDPE. Therefore, the polymer chain of PLA could move easily through the MMT interlayer. However, PP/LDPE/PLA/MMT composite with 5 phr MMT tended to have the agglomeration phenomena with decreased interlayer spacing compared with PP/LDPE/PLA with 3 phr MMT.
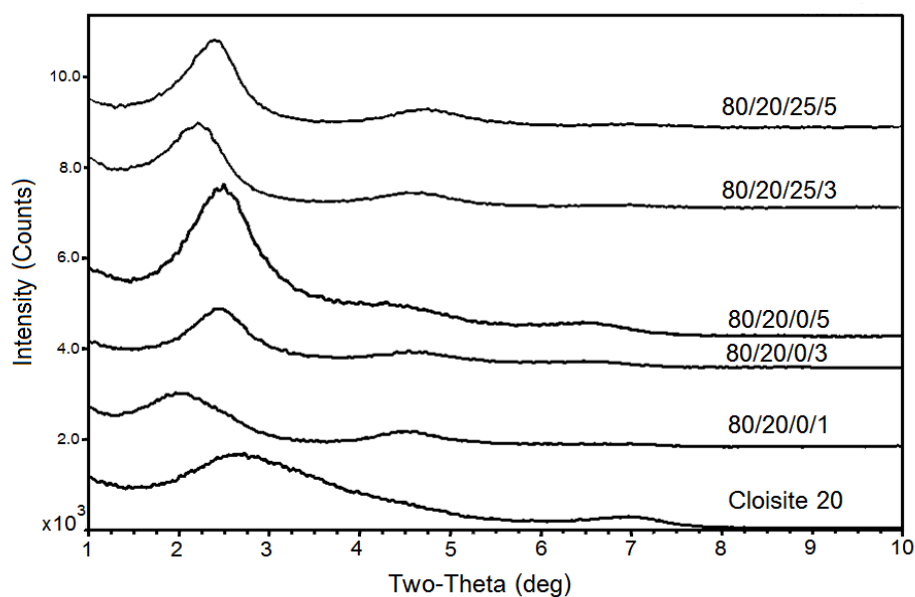
Figure 4.10 XRD patterns of PP/LDPE/PLA/MMT composite films at various

PLA and MMT loading.

Table 4.9 X-ray diffraction angle and D_{001}-spacing of MMT in PP/LDPE/PLA/MMT composite films

Sample code*	X-ray diffraction angle (2θ $^\circ$)	D_{001}-spacing between clay platelet (nm)
Cloisite 20	2.73	3.23
80/20/0/1	2.04	4.33
80/20/0/3	2.42	3.65
80/20/0/5	2.50	3.53
80/20/25/3	2.21	3.99
80/20/25/5	2.39	3.69

*a/b/c/d denoted the phr of PP, LDPE, PLA and MMT, respectively.

4.2.5 Permeability properties

The permeable properties of PP/LDPE/PLA/MMT composite films were evaluated in terms of oxygen transmission rate (OTR) and water vapor transmission rate (WVTR) and the results are presented in Table 4.10 and Figure 4.11a-b. From the Figure 4.11a, Blending of 80/20 PP/LDPE with 25 phr of PLA led to a 50% decrease in OTR (from 2098.7 cc/m^2·day of 80/20/0 to 1009.7 cc/m^2·day of 80/20/25), but addition of 35 phr of PLA led to dramatic increase in OTR (4157.5 cc/m^2·day of 80/20/35/0) that was much higher than PP/LDPE blend film. The lower oxygen permeability value of 80/20/25 PP/LDPE/PLA blend was attributed to the optimum size of PLA droplet that had function as oxygen barrier in the blends and gave the increased tortuosity of permeant path, while blend 80/20/35 PP/LDPE/PLA provided the agglomerate of PLA leading to the lower dispersion of PLA in PP matrix that the oxygen could easily diffuse in PP phase [3].

Considering the effect of MMT on the oxygen permeation, the OTR value was decreased with increasing MMT. Besides, the PP/LDPE/PLA/MMT composite films exhibited the lower OTR than PP/LDPE/PLA and PP/LDPE/MMT films, indicating that MMT (3-5 phr) improved the compatibility between PP and PLA. Moreover, PLA (20 phr) could enhance the interlayer spacing leading to the tortuosity of oxygen permeant path (Figure 4.12) [3].

From Table 4.10, the water vapor transmission rate (WVTR) of 80/20/35 PP/LDPE/PLA blend (4.47 g/m^2·day) was higher than the 80/20 PP/LDPE blend (3.14 g/m^2·day) The WVTR of blend was increased with increasing PLA content because PLA was polar polymer with relatively high value of water vapor permeability. However, the WVTR of composite films was decreased with MMT addition (from 3.90 g/m^2·day of 80/20/25/0 to 3.60 g/m^2·day of 80/20/25/5). This MMT addition affected the increased tortuous path in Intercalation and exfoliation of silicate layer leading to the decreased water vapor permeation. Therefore, the 80/20/25/3 PP/LDPE/PLA/MMT composite film was selected to study the tomato packaging storage and biodegradation because the mechanical, optical and permeability properties were better than other composite films.

Table 4.10 Oxygen transmission rate and water vapor transmission rate of
PP/LDPE/PLA/MMT composite films

PP/LDPE/PLA/MMT*	OTR (cc/m^2·day)	WVTR (g/m^2·day)
100/0/0/0	1689.6	3.10
80/20/0/0	2098.7	3.14
80/20/25/0	1009.7	3.90
80/20/35/0	4157.5	4.47
80/20/0/1	2087.6	3.08
80/20/0/3	1613.7	3.07
80/20/0/5	1356.2	3.07
80/20/25/3	939.2	3.82
80/20/25/5	917.7	3.60

*a/b/c/d denoted the phr of PP, LDPE, PLA and MMT, respectively.
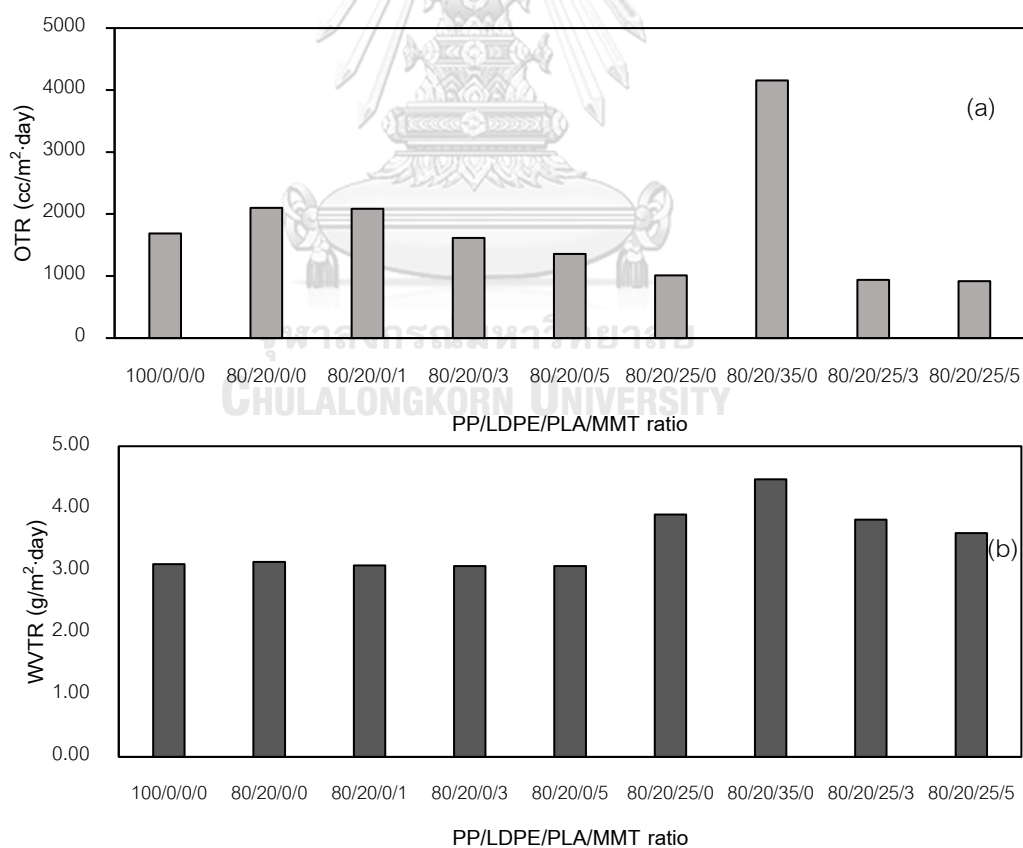
Figure 4.11 Effect of PLA and MMT content on the permeability properties of
PP/LDPE/PLA/MMT composite films (a) OTR and (b) WVTR.
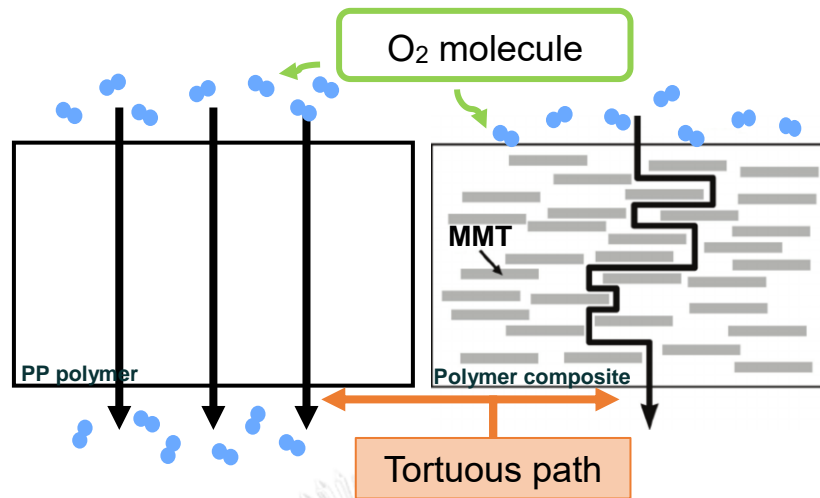
Figure 4.12 Comparison of the tortuosity of oxygen permeant path.

4.3 Morphology of blends

The surface morphology of PP, PP/LDPE and PP/LDPE/PLA blends is shown in Figure 4.13a-d. The blend morphology displayed the heterogeneous phase with the arrangement of polymer phase according to MD. Thus, the PP/LDPE and PP/LDPE/PLA blends were the immiscible blend. The PP/LDPE/PLA blend morphology (Figure 4.13c-d) exhibited the PLA spherical domains, representing in the light part dispersed in the PP/LDPE matrix of blends. This could be seen evidently by oxygen mapping as shown in the Figure 4.14a-b. The PP/LDPE blend with 25 phr PLA exhibited the uniformly dispersed oxygen, while the blend with 35 phr PLA had a slight tendency to form the agglomerated PLA particles. The agglomerates could be attributed to the phase separation, which caused the easily break of film and increased OTR.
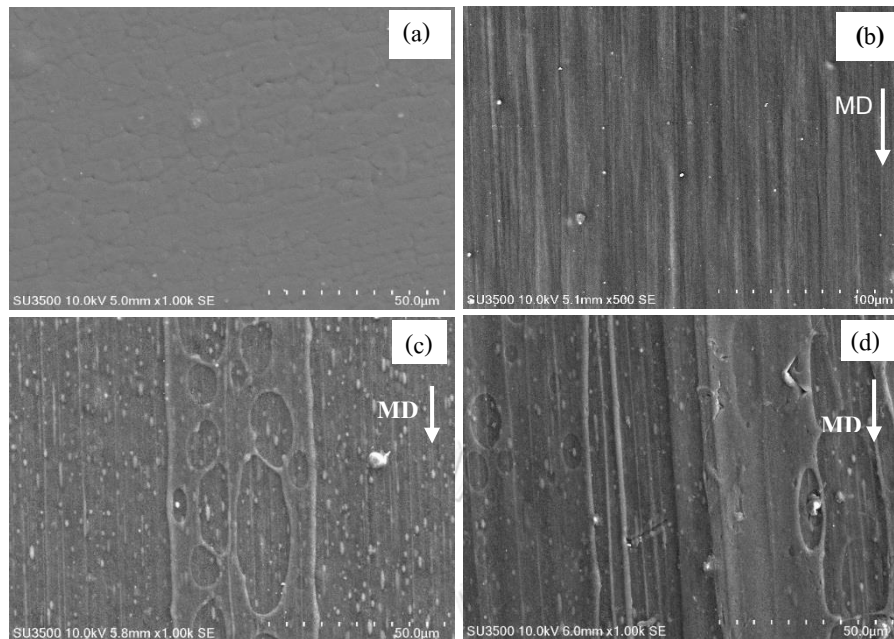
Figure 4.13 Representative SEM image of PP/LDPE/PLA blend films: (a) 100/0/0,

(b) 80/20/0 (c) 80/20/25 and (d) 80/20/35 (X1000 magnification).
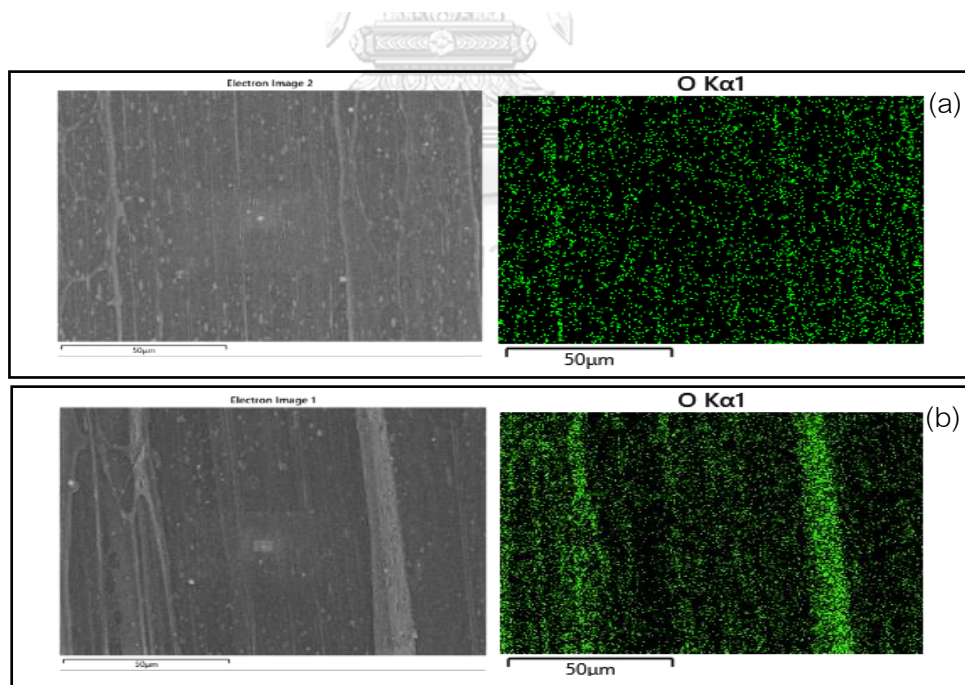
Figure 4.14 Representative SEM-EDS elemental mapping of PP/LDPE/PLA blend films:

(a) 80/20/25 and (b) 80/20/35.

Transmission Electron Microscopy (TEM) images of PP/LDPE/MMT composite films are shown in Figure 4.15a-c and a'-c'. The clay platelets appeared in good dispersion and random orientation in polymer matrix. However, the composite film that with 5 phr MMT exhibited the agglomeration of particles. Considering the 175000X of magnification (Figure 4.15a'-c'), the clay dispersed with the clay tactoids and intercalation formation and it was the evident that confirmed the increased interlayer of clay.

For the PP/LDPE/PLA/MMT composite films, clay particle displayed the better dispersion than composite films without PLA (Figure 4.15a-b and a'-b'). Most clay particles were located in the interface between PP or LDPE matrix and PLA, implying that clay particle could act as the compatibilizer between PP or LDPE matrix and PLA, that evidenced in the increased elongation at break of PP/LDPE/PLA with adding MMT. Besides, the TEM images at 44000X magnification shows more intercalation and exfoliation than PP/LDPE/MMT composite films (Figure 4.15a'-b') denoted that PLA adding had the role in the increased interlayer spacing of clay.
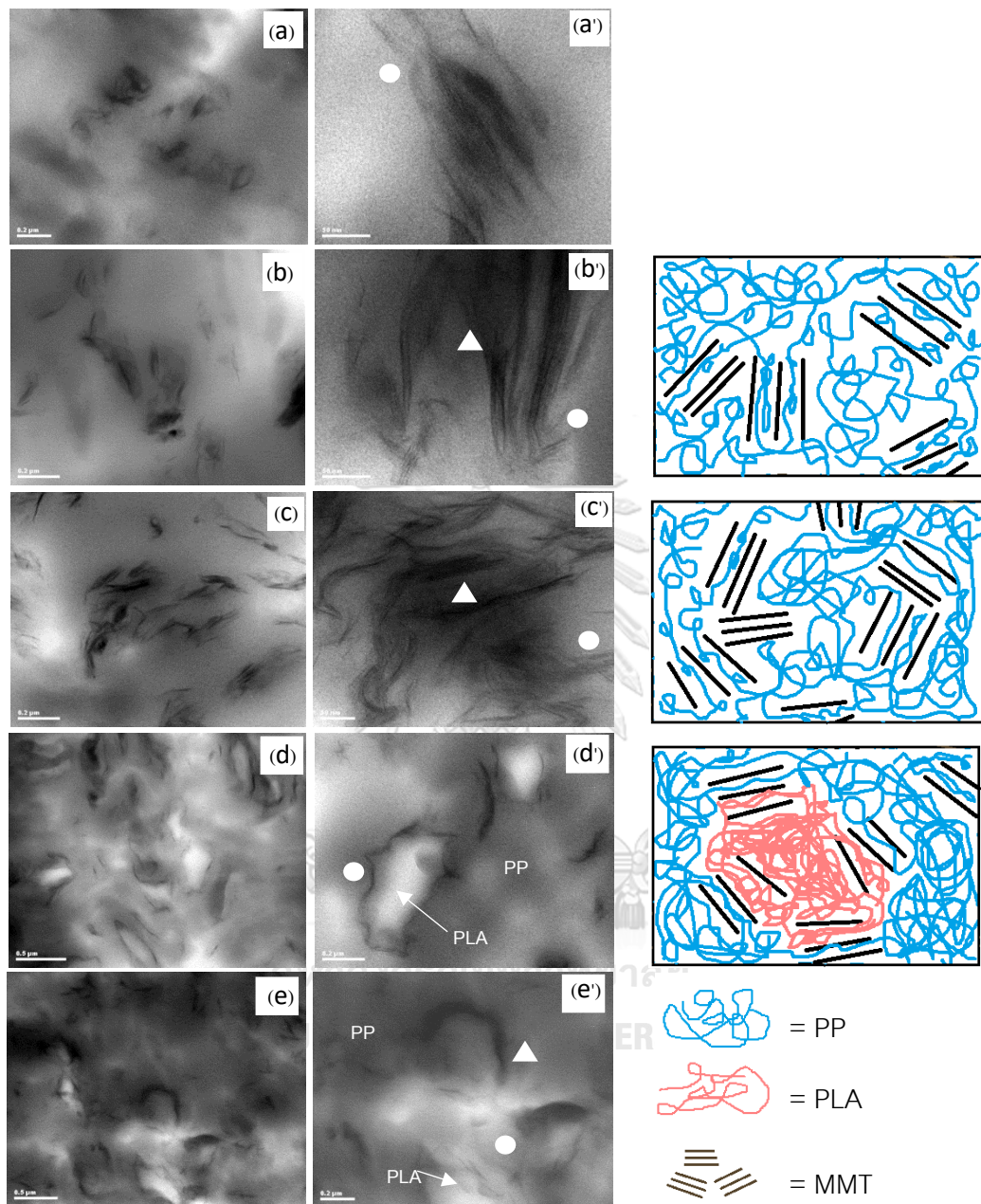
Figure 4.15 Representative TEM image PP/LDPE/PLA/MMT composite films: (a, a')
80/20/0/1, (b, b') 80/20/0/3, (c, c') 80/20/0/5, (d,d') 80/20/25/3 and (e,e' 80/20/25/5) by
a, b, c, d' and e' = 44000X magnification, a', b' and c' = 175000X magnification, and d
and e = 25500X magnification.

● = intercalate formation, ▲ = aggromeration

4.4 Physiological loss weight and appearance of tomato

The weight loss in tomato was observed during storage due to loss in moisture content as shown in Table 4.11 and Figure 4.16. The control tomato had 12.3% of weight loss followed by tomato in PP film (2.46%), 80/20/25/3 film (2.33%) and commercial film (1.90%) after 45 storage day at 14-20 ℃. Considering the rate of loss weight, the tomato in 80/20/25/3 film had higher weight loss than in commercial film and lower than in PP film (Figure 4.16). The tomato in 80/20/25/3 PP/LDPE/PLA/MMT film showed the lower rate of loss weight than PP film due to the low oxygen permeability of the package led to retardation of physiological process such as respiration and metabolic process of tomato during storage. While the commercial film gave the least weight loss of tomato because it might be the multi-layer film, oriented polypropylene film, or biaxially oriented polypropylene film.

The appearance of tomato at the initial time and during storage at 15, 30, and 45 days is shown in Figure 4.17a-d. The appearance of control tomato (unpacked tomatoes) changed from firmness to wrinkled skin as a signal of the dehydration after 30 days of storage (Figure 4.17a), meanwhile, the tomato in PP film showed a slightly wrinkled skin after 45 storage days (Figure 4.17b). The packaging in 80/20/25/3 and commercial films, the tomato appearance remained firm after 45 storage days (Figure 4.17c-d). This result confirmed that the moisture loss of tomato in 80/20/25/3 and commercial films was lower than that in PP film. However, the color of tomato packed with PP film and composite film became red, increasing red from the initial, while tomato packed in commercial film was still an orange-red color after 45 storage days, implying that oxygen could permeate the PP and 80/20/25/3 PP/LDPE/PLA/MMT composite film more than commercial film that led to accelerate the ripening process of tomato.

Table 4.11 Effect of packaging material on the physiological loss weight of tomato

Storage periods	Weight loss (%)			
	Control	PP film	80/20/25/3* film	Commercial film
3 days	0.94±0.16	0.38±0.13	0.11±0.04	0.16±0.02
6 days	1.91±0.28	0.64±0.17	0.35±0.27	0.24±0.02
9 days	2.75±0.40	0.74±0.15	0.58±0.30	0.44±0.07
13 days	3.92±0.55	1.04±0.25	0.67±0.28	0.54±0.04
15 days	4.73±0.71	1.22±0.26	0.79±0.23	0.65±0.01
21 days	5.99±0.88	1.43±0.42	1.08±0.20	0.92±0.11
24 days	6.51±0.97	1.50±0.40	1.21±0.20	1.04±0.13
27 days	7.65±1.1	1.57±0.39	1.44±0.26	1.14±0.12
30 days	8.36±1.2	1.72±0.34	1.54±0.31	1.20±0.10
39 days	10.4±1.6	1.94±0.38	1.92±0.36	1.72±0.30
45 days	12.3±1.8	2.46±0.07	2.33±0.39	1.90±0.27

*80/20/25/3 represent the phr of PP/LDPE/PLA/MMT composite film
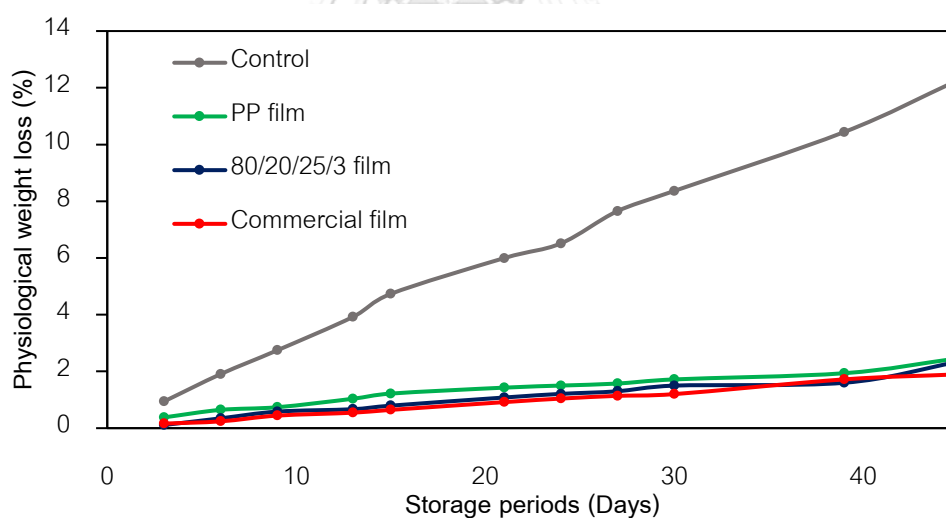
Figure 4.16 Change in %PLW of tomato storage with various films under 14-20 ℃ storage.
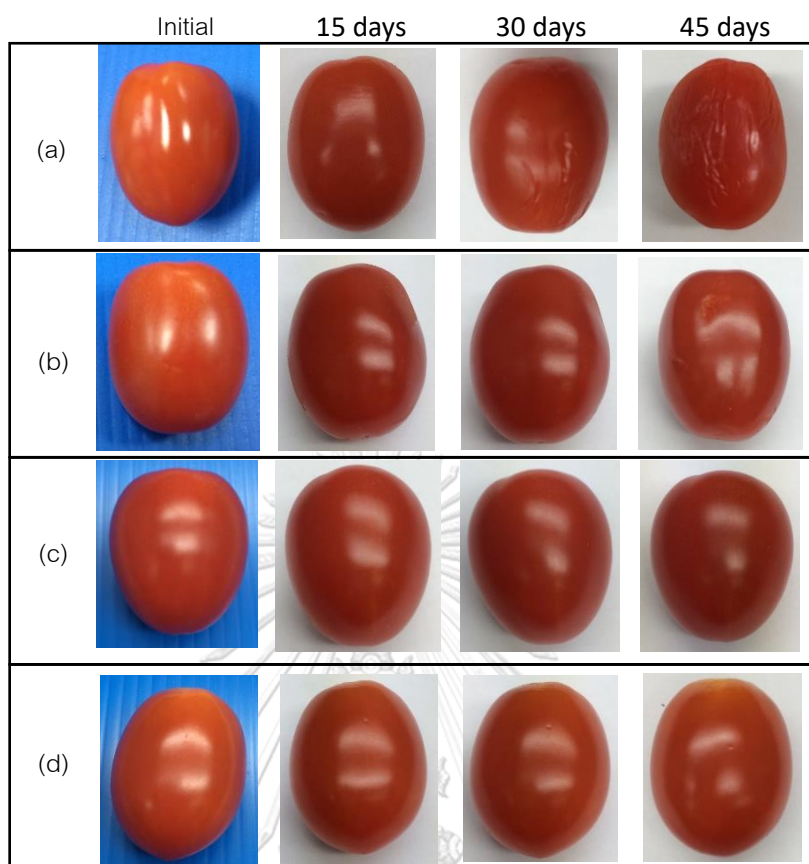
Figure 4.17 Appearance of tomato in different films for initial, 15, 30, and 45 days: (a) Control tomato, (b) PP film, (c) 80/20/25/3 film and (d) commercial film.

4.5 Biodegradation

The loss weight of film after burial test in the natural soil(34 °C and 90% RH) for 15, 30, 60 and 90 days is presented in Table 4.12. The decrease in weight of the 80/20/25/3 films was 0.94% of the initial weight, while the weight PP, LDPE and commercial film did not change at 90 days. The appearance of PP/LDPE/PLA/MMT films did not change after burial test in the soil for 90 days due to the less PLA content (20 phr) in PP and LDPE matrix and the good interface adhesion of MMT addition (Figure 4.18). The tensile strength, elongation at break and tensile modulus in MD of film are presented in Table 4.13 and Figure 4.19a-c. The tensile strength, elongation at break and tensile modulus of 80/20/25/3 PP/LDPE/PLA/MMT film were slightly decreased during the 30-90 days burial period (from 23.9 MPa of initial to 20.2 MPa of 90 days) but

the PP, LDPE and commercial films did not significantly change. The decreased tensile strength and tensile modulus implied that PLA structure might be degraded by the hydrolysis reaction of the biodegradation. Therefore, the film weight and the decreased tensile properties of 80/20/25/3 PP/LDPE/PLA/MMT film showed the related results which indicating that the composite film degraded during burial test in the soil due to the presence of PLA.

Table 4.12 The loss weight (%) of film after 15, 30, 60 and 90 days of soil burial test

Sample	Weight loss (%)			
	15 days	30 days	60 days	90 days
PP film	0	0	0	0
LDPE	0	0	0	0
80/20/25/3 film	0.22	0.47	0.89	0.94
Commercial film	0	0	0	0

*80/20/25/3 represent the phr of PP/LDPE/PLA/MMT composite film

	Initial	15 days	30 days	60 days	90 days
PP film					
LDPE film					
PP/LDPE/PLA/MMT film					
Commercial film					
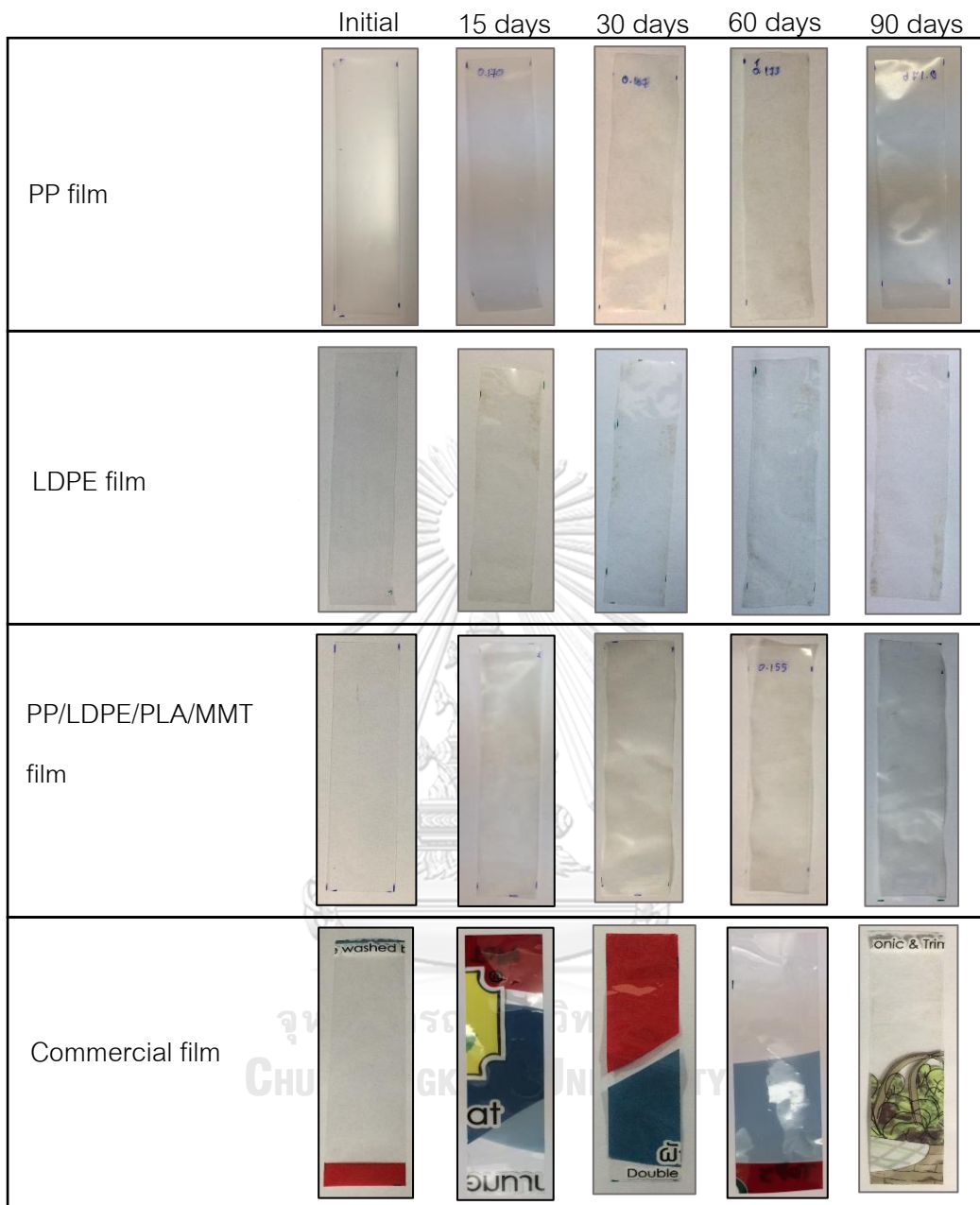
Figure 4.18 Appearance of films at initial, 15, 30, 60 and 90 days after burial test in the soil.

Table 4.13 The mechanical properties of films after 15, 30, 60 and 90 days of soil burial test

Film type	Burial period	Tensile strength (MPa)	Elongation at break (%)	Tensile modulus (MPa)
PP	Initial	32.5±1.0	480±20	941±32
	15 days	33.2±1.0	480±22	914±12
	30 days	32.9±1.8	480±7	933±19
	60 days	33.3±1.4	470±19	922±15
	90 days	32.4±0.7	470±16	933±19
	150 days**	32.4	470	930
LDPE	Initial	13.8±0.5	150±8	139±7
	15 days	13.5±0.9	140±8.	138±6
	30 days	13.4±1.2	150±10	136±6
	60 days	13.8±0.7	140±8	139±2
	90 days	14.2±0.9	140±24	143±6
	150 days**	14.2	140	143
80/20/25/3 film*	Initial	23.9±0.5	380±5	1890±87
	15 days	22.0±1.9	350±17	1858±31
	30 days	21.4±1.2	350±24	1705±22
	60 days	20.5±1.3	350±11	1665±27
	90 days	20.2±0.6	320±5	1625±49
	150 days**	17.9	280	1600
Commercial film	Initial	45.3±2.2	56±5	2297±49
	15 days	44.9±4.1	56±2	2333±114
	30 days	44.7±3.5	57±7	2274±80
	60 days	45.2±2.2	63±6	2286±88
	90 days	45.6±1.3	50±5	2334±96
	150 days**	45	55	2330

*80/20/25/3 represent the phr of PP/LDPE/PLA/MMT composite film

**by extrapolation
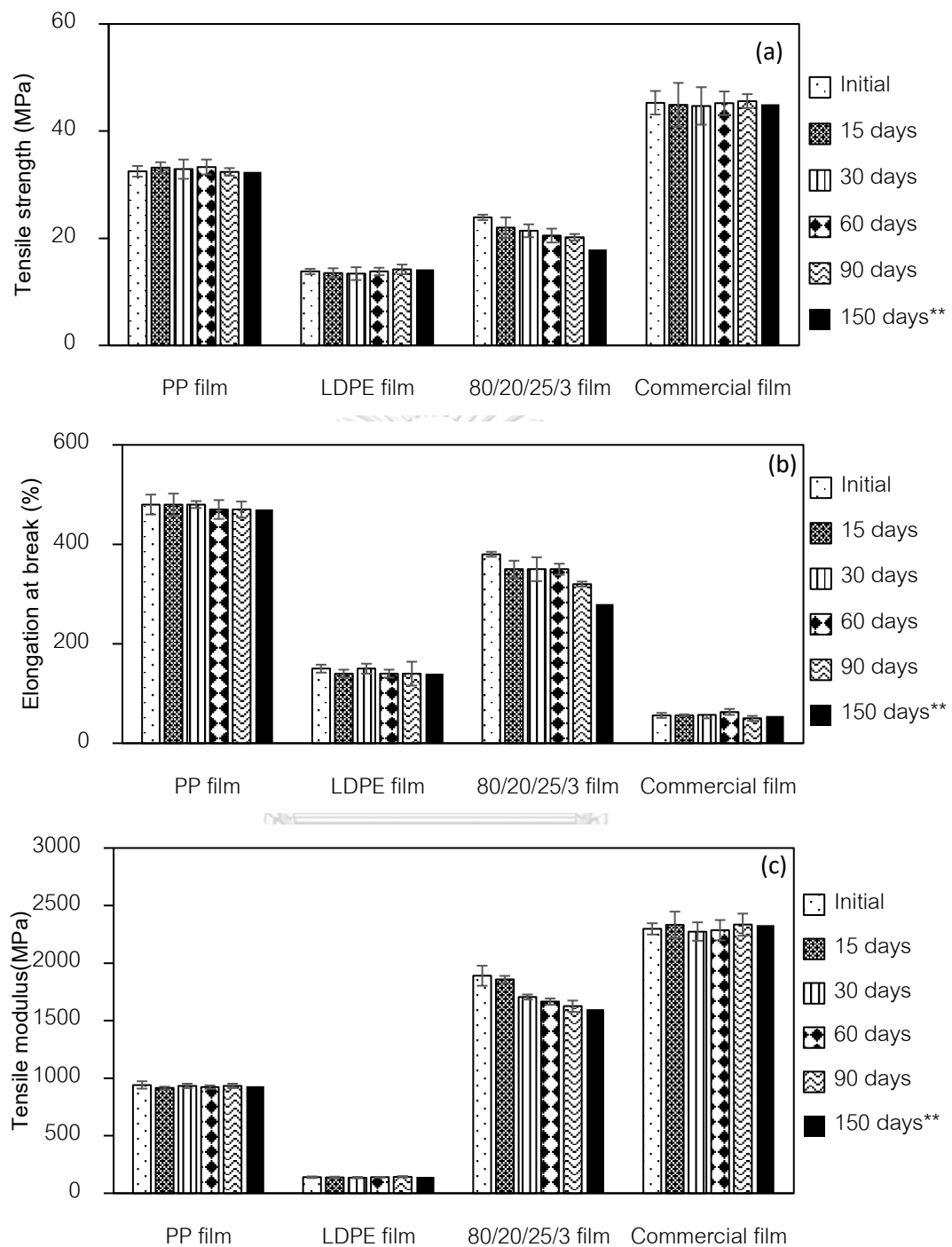
Figure 4.19 The mechanical properties of films after 15-90 days of soil burial test

(a) Tensile strength, (b) Elongation at break, and (c) Tensile modulus

**by extrapolation

4.6 Cost estimation of blend

The cost was estimated by using the raw material price, including PP, LDPE, PLA and MMT as summarized in Table 4.14. The estimated cost can be used to select the appropriate blend which is the balance in cost and film properties. The 80/20/25/3 PP/LDPE/PLA/MMT composite film presented the high material cost when compared to PP or LDPE film. However, the composite film could be the material for the single layer barrier film that was not complex processing. Moreover, the finished film product could be recycled for reducing waste amount.

Table 4.14 Summary estimated cost of blends

Formulation Name	Cost (bath/kg)
PP	39
LDPE	49
80/20 PP/LDPE	41
80/20/25 PP/LDPE/PLA	68.5
80/20/25/3 PP/LDPE/PLA/MMT	78.1

Remark: PP, LDPE, PLA and MMT cost are 39, 49, 110 and 320 baht/kg, respectively.

CHAPTER V

Conclusion

5.1 Conclusion

The effect of PP, LDPE, PLA and montmorillonite composition on mechanical properties, thermal properties and permeability of composite film were investigated. In this work, the appropriate blend formulation was obtained for balancing the mechanical and permeability properties for food packaging application. From the results, could be concluded as follows;

1. For PP/LDPE blend, LDPE could enhance the flexible and tear resistance properties. The addition 20 wt% LDPE in PP blend did not significantly affect the tensile modulus and tensile strength. For thermal properties, the LDPE addition (10-20 phr) has no significant effect on melting temperature but the crystallinity of PP was decreased with increasing LDPE content. However, the thermal stability of blend at various ratios did not change.

2. For PP/LDPE/PLA blend, the mechanical properties depended on the dispersion of PLA and interface adhesion between PLA and PP or LDPE. PLA could enhance the stiffness and oxygen barrier properties but decreased the tear resistance, thermal stability and water vapor barrier properties. The addition of 25 phr PLA in 80/20 PP/LDPE blend gave the good balance of mechanical and barrier properties.

3. The compatibility of 80/20/25 PP/LDPE/PLA blend could be improved by MMT addition, resulting the improved tear resistance, thermal stability, and barrier properties of films. The addition of 3 phr MMT in composite film gave the good dispersion and balancing the mechanical and barrier properties.

4. The transparency of blend film slightly decreased with increasing LDPE and PLA content because of the immiscibility of blend. Moreover, the increasing MMT content led to decrease the transparency due to the agglomeration of nanoparticles.

5. The physiological weight loss of tomato packed in the PP/LDPE/PLA/MMT composite film was lower than that in PP film with storage up to 45 days, so this composite film could be the alternative for the extended shelf life of tomato and the biodegradable material.

5.2 Suggestion for Future Work

1. The MMT could improve the compatibility between PLA and PP or LDPE, therefore, the increasing PLA content (30-40 phr) of film should be further studies for the increasing the ability of biodegradation.

2. The properties of food packaging composite produced by other process such as blown film extrusion, injection molding, and thermoforming should be investigated.

REFERENCES

1.   Kadhim, L. F.; Kadhim, Z. F. Studying the properties of PP/LDPE polymer blend. *Engineering Science.* **2017**, *25*, 193-201.

2.   Mofokeng, T. G.; Ojijo, V.; S., R. S. Influence of blend ratio on the morphology, mechanical, thermal, and rheological properties of PP/LDPE blends. *Macromolecular Materials and Engineering.* **2016**, *302*, 1191-1201.

3.   Ebadi-Dehaghani, H.; Barikani, M.; Khonakdar, H. A.; Jafari, S. H.; Wagenknecht, U.; Heinrich, G. On oxygen gas permeability of PP/PLA/clay nanocomposites: A molecular dynamic simulation approach. *Polymer Testing.* **2015**, *45*, 139-151.

4.   Ebadi-Dehaghani, H.; Khonakdar, H. A.; Barikani, M.; Jafari, S. H. Experimental and theoretical analyses of mechanical properties of PP/PLA/clay nanocomposites. *Composites: Part B* **2015**, *69*, 133-144.

5.   Devesh, T., *Practical guide to polypropylene.* Fist Published: United Kingdom, 2002.

6.   The Essential Chemical Industry. Polyethylene. http://www.essentialchemicalindustry.org/polymers/polyethene.html. (accessed 2018 Dec 8).

7.   Cormelia, V.; Mihaela, P., *Practical guide to polyethylene.* iSmithers Rapra Publishing: United Kindom, 2005.

8.   Rafael, A. A.; Loong-Tak, L.; Susan, E. M.; Selke, E. M.; Hideto, T., *Poly(lactic acid): Synthesis, Structures, Properties, Processing, and Application.* John Wiley&Sons, : Canada, 2010.

9.   IIT Delhi. Fibres for medical application. https://nptel.ac.in/courses/116102006/module6/chapter%206.1.html. (accessed 2018 Dec 8).

10.   LLC, U. Polylactic acid (PLA) Typical Properties. https://plastics.ulprospector.com/generics/34/c/t/polylactic-acid-pla-properties-processing

(accessed 2018 Dec 8).

11.   Bibi, I.; Icenhower, J.; Niazi, N. K.; Naz, T.; Shahid, M.; Bashi, S. Clay mineral: Structure, chemistry, and significance in contaminated environments and geological CO_2 sequestration. *Environment Material and Waste.* **2016**, 543-567.

12.   Marchuk, S. The dynamics of potassium in some Australian soils. University of Southern Queensland, 2016.

13.   Charles, E. W.; Lin, D. P., *The Chemistry of Clay Minerals*. Elsevier Scientific: New York, 1975; Vol. 15.

14.   Aphiwantraku, S. Synthesis and characterization of polymer-clay nanocomposite. Mahidol University, 2002.

15.   David, R. S. Texture evolution in processing of polystyrene-clay nanocomposites. Drexel University, 2007.

16.   Kampeerapappun, P. Preparation of cassava starch/montmorillonite nanocomposite film. Chulalongkorn University, 2003.

17.   Jorge, V. F. L. C.; Cesar, A. M. A.; Marilda, N. C.; S., M. A. M.; Mohand, B.; Osmas, S. B. Removal of effluent from petrochemical wastewater by adsorption using organoclay. *Petrochemica.* **2012**, 277-294.

18.   Gordon, L. R., *Food Packaging Principle and Practice*. John Wiley&Sons: Boca Raton, 2013.

19.   Pinnavaia, T. J.; Beall, G. W., *Polymer-clay Nanocomposites*. John Wiley&Sons: England, 2000.

20.   Sabu, T.; Yves, G.; Jyotishkumar, P., *Charecterization of Polymer Blends: Miscibility, Morphology and Interface.* John Wiley&Sons: United State of America, 2014.

21.   Polymer Science Learning Center. Immiscible Polymerr Blends. https://www.pslc.ws/macrog/iblend.htm (accessed 2018 Dec 13).

22.   Gabriel, O. S.; George, P. S., *Polymer Blends and Alloys*. Marcle Dekker: New York, 1999.

23.   Donald, G. B.; Dimitris, I. C., *Polymer Processing and Principles and Design*. John Wiley&Sons: Canada, 1998.

24.   Wilkinson, A. N.; Ryan, A. J., *Polymer Processing and Structure Development*. Kluwer Academic Publishers: Netherland, 1998.

25.   Chang, A. C.; Tau, L.; Hiltner, A.; Baer, E. Structure of blown film from blends of polyethylene and high melt strength polypropylene. *Polymer.* **2002**, *43*, 4923-4933.

26.   Abdel-Hamid, I. M. Thermo-mechanical characteristics of thermally aged polyethylene/polypropylene blends. *Materials and Design.* **2010**, *31*, 918-929.

27.   Pivasaart, S.; Kordsaard, J.; Pivsaart, W.; Wongpajan, R.; Ocharoen, N.; Pavasupree, S.; Hamada, H. Effect of compatibilizer on PLA/PP blend for injection molding. *Energy Procedia.* **2016**, *89*, 353-360.

28.   Pannirselvan, M.; Genovese, A.; Jollands, M. C.; S.N., B.; Shanks, R. A. Oxygen barrier property of polypropylene-polyether treated clay nanocomposite. *Express Polymer Letters.* **2008**, *2*, 429-439.

29.   Girdthep, S.; Worajittiphon, P.; Molloy, R.; Lumyong, S.; Leejarkpai, T.; Punyodom, W. Biodegradable nanocomposite blown films based on poly(lactic acid) containing silver-loaded kaolinite: A route to controlling moisture barrier property and silver ion release with a prediction of extended shelf life of dried longan. *Polymer.* **2014**, *55*, 6776-6788.

30.   Espinosa, K. R.; Castillo, L. A.; Barbosa, S. E. Blown nanocomposite films from polypropylene and talc, Influence of talc nanoparticles on biaxial properties. *Materials & Design.* **2016**, *111*, 25-35.

31.   Nouri, M.; Morshedian, J.; Rabbani, A.; Ghasemi, I.; Ebrahimi, M. Investigation of LLDPE/LDPE blown films by response surface methodology. *Iranian Polymer Journal.* **2006**, *15* (2), 155-162.

32.   Battegazzore, D.; Bocchini, S.; Frache, A. Crystallization kinetics of poly(lactic acid)-talc composites. *Express Polymer Letters.* **2011**, *5* (10), 849-858.

33.   Samper, M. D.; Bertomeu, D.; Arrieta, M. P.; Ferri, J. M.; Lopez-Martinez, J. Interference of biodegradable plastics in the polypropylene recycling process. *Materials.* **2018**, *11*, 1186-1204.

34.   Dong, Y.; Bhattacharyya, D. Investigation on the competing effects of clay

dispersion and matrix plasticisation for polypropylene/clay nanocomposites. Part I: Morphology and mechanical properties. *Journal of Material Science.* **2012**, *47*, 3900-3912.

APPENDIX

Table A-1 Tensile strength, elongation at break, tensile modulus and tear strength of PP/LDPE/PLA/MMT in MD and TD

PP/LDPE/PLA/MMT	MD				TD			
	TS (MPA)	EB (%)	TM (MPa)	Tear strength (kgf/cm)	TS (MPA)	EB (%)	TM (MPa)	Tear strength (kgf/cm)
	34.1	400	1123	16.7	27.5	390	1001	42.1
	33.6	390	1068	20.0	26.8	420	969	43.1
100/0/0/0	35.8	380	1045	16.7	27.8	420	964	48.5
	33.6	410	1047	17.2	28.7	400	1031	45.7
	33.1	430	1058	18.3	26.2	430	948	40.5
Average	34.0	400	1068	17.8	27.4	410	983	44.0
SD	1.0	19	32	1.42	1.0	11.0	33	3.17
	32.9	490	944	17.5	21.3	380	915	38.8
	35.5	510	964	14.2	23.8	390	929	37.8
90/10/0/0	33.8	480	990	19.0	23.6	400	931	37.7
	32.8	480	996	14.6	23.7	380	871	37.6
	35.8	460	1008	17.7	22.8	380	890	38.9
Average	34.2	480	980	16.6	23.0	390	907	38.1
SD	1.4	18	26	2.07	1.1	9	26	0.63
	35.9	530	996	13.4	21.7	340	890	47.0
	35.0	490	927	11.8	21.5	330	839	45.3
85/15/0/0	34.7	470	924	11.0	20.2	350	863	47.8
	34.5	460	942	10.1	22.0	370	923	48.6
	34.2	490	973	12.4	20.5	330	891	46.5
Average	34.9	490	952	11.7	21.2	350	881	47.0
SD	0.7	18	31	1.25	0.8	17	32	1.25

TS = Tensile strength, EB = Elongation at break and TM = Tensile modulus

PP/LDPE/PLA/MMT	MD				TD			
	TS (MPA)	EB (%)	TM (MPa)	Tear strength (kgf/cm)	TS (MPA)	EB (%)	TM (MPa)	Tear strength (kgf/cm)
	33.0	480	969	10.4	20.4	330	836	45.2
	32.6	470	921	10.7	20.5	330	898	44.6
80/20/0/0	31.1	480	941	8.92	21.5	330	896	50.1
	34.9	480	953	11.0	19.0	330	829	44.7
	33.6	480	954	6.57	18.8	290	855	49.3
Average	33.0	470	948	10.7	20.0	320	863	44.8
SD	1.4	4	18	0.3	1.1	18	33	0.33
	13.7	150	135	27.4	9.1	307	135	42.6
	13.3	160	146	27.7	7.9	284	129	41.4
0/100/0/0	13.3	140	137	28.6	6.9	246	127	42.1
	14.1	150	147	26.2	9.5	324	139	42.6
	14.6	160	139	28.3	6.1	217	127	42.5
Average	13.8	150	139	27.6	7.9	290	131	42.2
SD	0.5	8	2	1.0	1.5	34	5	0.50
	34.4	320	1534	1.61	11.8	1.6	1061	23.4
	35.0	350	1665	1.28	13.0	1.9	1070	25.6
80/20/25/0	34.4	330	1552	1.33	12.7	2	1077	21.9
	34.5	350	1539	1.29	12.3	1.8	1096	22.9
	34.2	340	1494	1.42	13.6	2	1094	22.6
Average	34.5	338	1556.8	1.38	12.7	1.9	1079.6	23.3
SD	0.30	13.04	64.25	0.14	0.68	0.17	15.18	1.4
	25.3	220	1717	0.92	9.1	9.1	1202	12.2
	25.4	210	1779	1.17	8.4	8.4	1203	11.7
80/20/35/0	23.5	220	1696	0,80	10.9	10.9	1306	11.6
	24.8	220	1792	0,85	11.3	11.3	1182	12.7
	23.9	210	1703	1.05	10.2	10.2	1236	9.36
Average	24.6	220	1737.4	0.96	10.0	10.0	1225.8	11.5
SD	0.83	5	44.79	0.15	1.24	1.24	48.84	1.3

TS = Tensile strength, EB = Elongation at break and TM = Tensile modulus

PP/LDPE/PLA/MMT	MD				TD			
	TS (MPA)	EB (%)	TM (MPa)	Tear strength (kgf/cm)	TS (MPA)	EB (%)	TM (MPa)	Tear strength (kgf/cm)
	33.2	460	1345	14.9	22.9	400	1005	69.7
	30.0	440	1430	17.5	23.2	400	960	67.6
80/20/0/1	35.6	500	1286	17.9	20.8	380	904	71.8
	32.3	460	1363	16.2	20.8	390	950	64.9
	33.4	490	1316	13.3	20.8	370	952	60.4
Average	32.9	470.0	1348.0	16.0	21.7	390.0	954.2	66.9
SD	2.02	24.49	54.37	1.89	1.24	13.04	35.91	4.44
	30.6	420	1465	5.66	19.5	360	931	67.3
	33.7	470	1356	4.73	21.3	370	1209	69.3
80/20/0/3	29.2	440	1354	4.45	20.3	360	1197	74.4
	32.1	480	1327	6.24	20.8	360	1210	64.8
	30.7	470	1273	5.41	22.3	370	1142	70.1
Average	31.3	460.0	1355.0	5.30	20.8	360.0	1137.8	69.2
SD	1.71	25.10	70.02	0.72	1.05	5.48	118.92	3.55
	29.6	460	1286	4.87	19.5	340	1155	69.0
	28.4	430	1247	4.96	19.7	340	1108	70.8
80/20/0/5	26.0	400	1183	4.78	17.8	310	1114	72.0
	30.5	460	1229	4.57	19.3	330	1113	61.4
	29.0	460	1211	4.94	18.0	320	1065	66.5
Average	28.7	440	1231.2	4.82	18.9	330.0	1111.0	68.0
SD	1.70	27	38.69	0.16	0.89	13.04	31.91	4.19
	23.2	370	1986	5.99	14.1	10	1642	68.6
	24.3	380	1837	6.98	15.5	13	1507	66.7
80/20/25/3	23.5	370	1980	5.66	14.6	9	1482	67.8
	24.1	380	1852	5.14	14.2	9	1619	66.1
	24.2	380	1797	6.61	15.9	12	1742	72.1
Average	23.9	380	1890	6.08	14.9	11	1598	68.3
SD	0.48	5	87	0.73	0.80	2	106	2.38

TS = Tensile strength, EB = Elongation at break and TM = Tensile modulus

PP/LDPE/PLA/MMT	MD				TD			
	TS (MPA)	EB (%)	TM (MPa)	Tear strength (kgf/cm)	TS (MPA)	EB (%)	TM (MPa)	Tear strength (kgf/cm)
	22.2	370	1966	6.47	15.8	10	1738	70.9
	20.4	350	1856	6.13	13.6	12	1595	69.8
80/20/25/5	21.6	360	1888	5.87	16.1	12	1675	71.8
	22.3	350	1934	5.76	15.9	11	1603	67.4
	21.4	330	1908	6.08	16.7	13	1772	70.0
Average	21.6	350	1910	6.06	15.6	12	1677	70.0
SD	0.77	15	42	0.27	1.18	1	79	1.65

TS = Tensile strength, EB = Elongation at break and TM = Tensile modulus
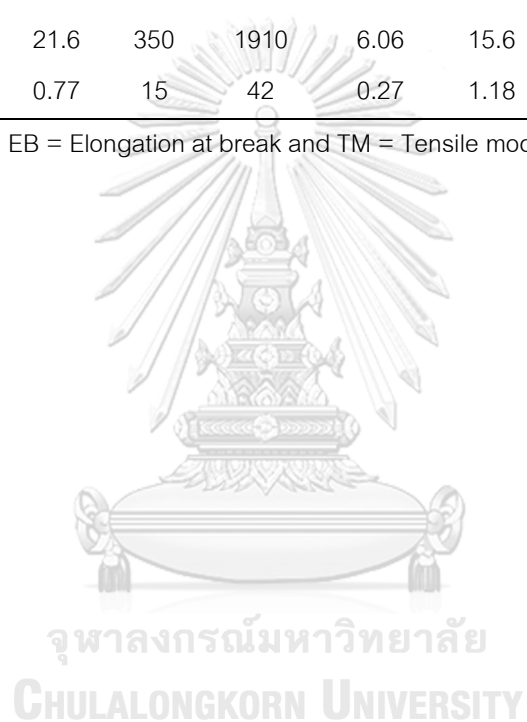
Table A-2 Effect of packaging materials on tomato physiological loss weight (g) over a storage period of 60 days at 14-20 ºC

Film type	Weight loss (%)										
	3 days	6 days	9 days	13 days	15 days	21 days	24 days	27 days	30 days	38 days	45 days
Control	0.76	1.62	2.35	3.42	4.11	5.20	5.65	6.67	7.29	8.98	10.62
	0.98	1.92	2.74	3.83	4.58	5.84	6.33	7.42	8.10	10.17	11.94
	1.08	2.18	3.15	4.52	5.50	6.94	7.56	8.87	9.70	12.17	14.23
Average	0.94	1.91	2.75	3.92	4.73	5.99	6.51	7.65	8.36	10.44	12.26
SD	0.16	0.28	0.40	0.55	0.71	0.88	0.97	1.12	1.23	1.61	1.83
PP film	0.43	0.83	0.90	1.32	1.51	1.91	1.95	2.02	2.11	2.38	2.45
	0.48	0.60	0.72	0.88	1.12	1.24	1.37	1.43	1.52	1.77	2.40
	0.23	0.50	0.60	0.91	1.03	1.14	1.19	1.27	1.53	1.66	2.54
Average	0.38	0.65	0.74	1.04	1.22	1.43	1.50	1.57	1.72	1.94	2.46
SD	0.13	0.17	0.15	0.25	0.26	0.42	0.40	0.39	0.34	0.38	0.07
80/20/25/3 composite film	0.09	0.18	0.39	0.47	0.57	0.91	1.11	1.29	1.33	1.62	2.07
	0.09	0.20	0.43	0.54	0.78	1.03	1.08	1.31	1.40	1.84	2.16
	0.15	0.66	0.93	0.99	1.03	1.31	1.43	1.74	1.90	2.31	2.78
Average	0.11	0.35	0.58	0.67	0.79	1.08	1.21	1.44	1.54	1.92	2.33
SD	0.04	0.27	0.30	0.28	0.23	0.20	0.20	0.26	0.31	0.36	0.39
Commercial film	0.19	0.26	0.49	0.59	0.65	0.95	1.09	1.15	1.25	1.75	1.95
	0.15	0.23	0.48	0.52	0.63	0.80	0.90	1.01	1.09	1.41	1.61
	0.15	0.23	0.36	0.52	0.65	1.00	1.15	1.25	1.26	2.00	2.14
Average	0.16	0.24	0.44	0.54	0.65	0.92	1.04	1.14	1.20	1.72	1.90
SD	0.02	0.02	0.07	0.04	0.01	0.11	0.13	0.12	0.10	0.30	0.27

Table A-3 The effect of natural soil burial on the loss weight (%) of film after 15, 30, 60 and 90 days

Film types	Periods	Initial weight (g)	After buried weight (g)	Weight loss (g)	Weight loss (%)	Weight loss average (%)
PP film	15 days	0.168	0.168	0	0	0
		0.173	0.173	0	0	
		0.170	0.170	0	0	
		0.166	0.166	0	0	
		0.170	0.170	0	0	
	30 days	0.168	0.168	0	0	0
		0.167	0.167	0	0	
		0.158	0.158	0	0	
		0.171	0.171	0	0	
		0.160	0.160	0	0	
	60 days	0.164	0.164	0	0	0
		0.169	0.169	0	0	
		0.173	0.173	0	0	
		0.167	0.167	0	0	
		0.172	0.172	0	0	
	90 days	0.165	0.165	0	0	0
		0.164	0.164	0	0	
		0.161	0.161	0	0	
		0.170	0.170	0	0	
		0.166	0.166	0	0	
80/20/25/3 composite film	15 days	0.185	0.183	0.002	1.08	0.27
		0.183	0.183	0	0.00	
		0.183	0.183	0	0.00	
		0.185	0.185	0	0.00	
		0.186	0.186	0	0.00	
	30 days	0.171	0.170	0.001	0.58	0.47
		0.184	0.184	0	0.00	
		0.153	0.152	0.001	0.65	
		0.183	0.181	0.002	1.09	
		0.194	0.194	0	0.00	
	60 days	0.180	0.178	0.002	1.11	0.89
		0.182	0.18	0.002	1.10	
		0.179	0.176	0.003	1.68	
		0.192	0.192	0	0.00	
		0.176	0.175	0.001	0.57	
	90 days	0.183	0.183	0	0	0.94
		0.166	0.163	0.003	1.81	
		0.180	0.178	0.002	1.11	
		0.164	0.162	0.002	1.22	
		0.171	0.170	0.001	0.58	

Film types	Periods	Initial weight (g)	After buried weight (g)	Weight loss (g)	Weight loss (%)	Weight loss average (%)
LDPE film	15 days	0.164	0.164	0	0	
		0.167	0.167	0	0	
		0.171	0.171	0	0	0
		0.169	0.169	0	0	
		0.165	0.165	0	0	
	30 days	0.171	0.171	0	0	
		0.171	0.171	0	0	
		0.164	0.164	0	0	0
		0.167	0.167	0	0	
		0.168	0.168	0	0	
	60 days	0.167	0.167	0	0	
		0.164	0.164	0	0	
		0.164	0.164	0	0	0
		0.169	0.169	0	0	
		0.166	0.166	0	0	
	90 days	0.167	0.167	0	0	
		0.167	0.167	0	0	
		0.174	0.174	0	0	0
		0.163	0.163	0	0	
		0.162	0.162	0	0	
Commercial film	15 days	0.141	0.141	0	0	
		0.141	0.141	0	0	
		0.144	0.144	0	0	0
		0.157	0.157	0	0	
		0.148	0.148	0	0	
	30 days	0.144	0.144	0	0	
		0.137	0.137	0	0	
		0.141	0.141	0	0	0
		0.139	0.139	0	0	
		0.145	0.145	0	0	
	60 days	0.157	0.157	0	0	
		0.144	0.144	0	0	
		0.144	0.144	0	0	0
		0.141	0.141	0	0	
		0.141	0.141	0	0	
	90 days	0.144	0.144	0	0	
		0.157	0.157	0	0	
		0.148	0.148	0	0	0
		0.149	0.149	0	0	
		0.143	0.143	0	0	

Table A-4 Tensile strength, elongation at break, and tensile modulus of films in MD after soil burial test

Film Type	TS (MPA)				EB (%)				TM (MPa)			
	15 days	30 days	60 days	90 days	15 days	30 days	60 days	90 days	15 days	30 days	60 days	90 days
PP	33.3	32.5	34.2	33.7	450	480	480	450	930	910	926	986
	32.9	35.2	35.2	33.2	460	490	480	490	910	958	934	981
	33.0	33.5	33.1	32.3	490	470	440	470	907	919	937	911
	34.2	33.0	31.6	31.8	500	480	490	480	900	945	900	921
	32.6	30.1	32.3	32.2	490	480	480	470	924	934	914	937
Average	33.2	32.9	33.3	32.4	480	480	470	470	914	933	922	947
SD	0.6	1.8	1.4	0.7	22	7	19	16	12	19	15	34
LDPE	14.3	14.7	14.6	14.4	130	140	130	130	143	144	138	135
	13.1	13.4	13.5	14.7	140	150	150	160	133	131	137	150
	14.2	14.6	13.2	14.7	130	160	140	150	140	130	141	146
	12.1	12.0	14.6	12.6	140	140	140	99	143	136	138	141
	13.9	12.5	13.2	14.5	150	160	150	150	130	139	143	143
Average	13.5	13.4	13.8	14.2	140	150	140	140	138	136	139	143
SD	0.9	1.2	0.7	0.9	10	10	8	24	6	6	3	6
80/20/25/3 Composite	22.9	20.3	21.9	20.6	340	360	340	330	1879	1698	1661	1652
	19.6	21.4	19.2	20.7	330	380	360	320	1868	1701	1645	1610
	24.7	20.3	21.4	20.4	370	330	370	320	1827	1719	1698	1555
	21.5	22.1	20.9	19.2	330	320	350	330	1823	1675	1634	1624
	21.3	23.1	19.1	20.2	350	360	350	320	1895	1734	1687	1685
Average	22.0	21.4	20.5	20.2	340	350	350	320	1858	1705	1665	1625
SD	1.9	1.2	1.3	0.6	17	24	11	5	32	22.4	27	49
Commercial Film	43.6	48.5	47.5	46.6	55	67	57	49	2320	2356	2254	2472
	42.5	43.1	44.7	45.0	58	48	69	52	2375	2267	2374	2365
	40.8	47.4	43.2	44.7	54	56	56	58	2155	2315	2384	2323
	48.2	42.5	42.6	47.5	55	53	64	43	2467	2289	2189	2302
	48.7	41.9	47.8	44.4	57	60	67	48	2346	2143	2237	2208
Average	44.8	44.7	45.2	45.6	56	57	63	50	2333	2274	2286	2334
SD	3.5	3.0	2.4	1.3	2	7	6	5	114	80	88	96

TS = Tensile strength, EB = Elongation at break and TM = Tensile modulus

VITA

NAME   Miss Supornpat Mooninta

DATE OF BIRTH   2 September 1992

PLACE OF BIRTH   Lampang, Thailand

INSTITUTIONS ATTENDED 2014 B.Sc. Chemistry, Faculty of Science, Chiang Mai
                       University, Thailand

                       2019 M.Sc. Petrochemistry and Polymer Science Program,
                       Faculty of Science, Chulalongkorn University, Thailand

HOME ADDRESS   192/4 Moo 7, Tambon Pong San Tong,
                       Muang, Lampang 52100, Thailand

PUBLICATION   June 13-14, 2019 The international Polymer Conference of
                       Thailand (PCT-9), Thailand

                       Proceeding:

                       Mooninta, S; Poompradum, S.; Prasassarakich, P., Improved
                       barrier properties of PP/LDPE composite film for packaging:
                       effect of montmorillonite and poly(lactic acid), Proceeding of
                       PCT-9, Bangkok, Thailand.